Fermilab

TM-1091
2972.0
ν 78

FURTHER DESIGN STUDIES FOR A TEVATRON ERA DICHROMATIC BEAM

THE NCI DICHROMATIC BEAM

Linda G. Stutte
February 17, 1982

Introduction

This report summarizes work done over the last year on a dichromatic beam design for a 1 TeV accelerator, in order to improve on existing designs[1], which suffered from a lack of acceptance.

The design described herein, the NCI beam design, is quite similar in form to the D-61G beam, described in reference 1. In particular, the six design goals mentioned in the above memo:

1. Reach secondary beam momenta up to x=3/4
2. Dump the non-interacting fraction of the primary proton beam cleanly in external dumps at all secondary momenta
3. Reduce the wide-band background component of the beam as much as possible (better or at least as well as the existing beam)
4. Obtain an energy resolution on individual events at a z location of the 15-foot bubble chamber (and for radial positions of up to one meter) of dE/E $\lesssim$ 10% for all secondary momenta
5. Obtain the highest flux of secondaries possible while keeping the momentum bite of the beam $<$ 10%

6. Contain the physical size (both longitudinal and transverse dimensions) of the beam layout in order to minimize costs.

will be discussed in turn and will be seen to be met by the NCI design.

As in all design efforts, some parameters must be optimized at the expense of others. The NCI design chooses to emphasize increased flux as the most important of the above list. As a consequence, wide-band background rejection and energy resolution at the detectors are worse than the D-61G design, but are still within the design goals. The justification for this optimization can be seen in Figure 1, taken from the E652 proposal, which shows the number of events expected per 10^{13} protons in the Lab E detector, for both neutrino and anti-neutrino running. The salient point from this figure is, that even with a multi-hundred ton detector, one can, at best, only expect an event per pulse,even with a theoretical "ideal beam" which gathers up most of the available flux. Thus, it is important to concentrate on good acceptance, to which the present design has been tailored.

Figure 2[2] shows the percentage of flux within a given production angle for a 10% momentum bite, for various secondary momenta. It has served as a figure of merit for this design effort. Past studies have shown that if one is containing 70% or so of the available flux in each of the two planes, for a total containment of 50%, one has achieved a reasonable solid angle acceptance. For a 750 GeV beam design, then, it is

reasonable to expect angular acceptances of 0.8-1.0 mr. As can easily be seen from the figure, however, this design criteria produces a poor acceptance at lower momenta, where particle production is at larger and larger angles. For example, at 300 GeV, one would need to contain almost 2.0 mr to achieve the same fractional acceptance. Since neutrino experiments do cover a range of secondary momenta, one then needs a range of beam designs which are optimized in terms of acceptance, for, as one sees from Figure 1, event rates are low no matter which momentum one chooses.

This design report has tried to address this problem, by providing a series of designs at various secondary momenta which all use the same bend points, in order to preserve the primary proton beam targetting positions and angles. This should lead to quick changeovers between the various options. The bend points have been fixed by the 750 GeV design. Then, at lower momenta, when some of the bending magnets are not needed, quadrupoles are added instead in order to increase the acceptance.

The NCI Design

A conceptual layout for the NCI 750 GeV beam design is shown in Figure 3. A detailed list of beam element positions and types is provided in Table A-1.

The major changes which have been made to the previous design are that the magnitudes of the bends have been reduced and the beam has been shortened. These changes have a variety of effects on the beam acceptance and geometry. First, by moving the quadrupoles closer to the target, the beam acceptance has improved. Because of this, the magnet apertures now do not remove all of the off-momentum and -angle rays, so that beam defining liners have to be placed in the first two magnets to clip these undesirable tails, resulting in a more critical alignment procedure. The liner in the first bending magnet is 1.0" full width in height and from -0.25" to +0.40" in widtn (the larger dimension being toward the east, the direction towards which the primary proton beam dumps). The liner in the second bending magnet is 2.0" full width in height and from -0.50" to +1.50" in width, with the same orientation as the first liner. Second, because the first bend string is smaller in magnitude than in previous designs, the non-interacting primary proton beam can exit the magnets and dump into external dumps (see Figure 4) without resorting to special aperture magnets. Third, since the first bend string is smaller in magnitude than the second string, the final bend string is rotated through a much smaller angle. Larger aperture bending magnets are no longer needed here in order to increase the acceptance. As a result of all this, the beam can be made entirely out of conventional magnets; 6-3-120 dipoles, 4Q-120 and 8NQ32A quadrupoles, at a large savings in cost. Finally, the lateral excursions of the beam have lessened, and consequently, the dichromatic beam and the triplet beam[3] can both be

mounted in roughly the same locations. This point will be discussed in further detail in the final section of this report.

The most important beam parameters are summarized as follows:

1. For dp/p = 0, the angular acceptance = 0.85 x 0.70 mr.

2. The momentum bite of the beam is 15.5% (flat production spectrum) or 8% (production model used).

3. The final divergence of the beam in the decay pipe is 0.09 mr.

The incoming proton beam targets at 3.62mr and -6.08mr, respectively, in the vertical and horizontal directions. It is important to have a slight vertical angle in the secondary beam while the horizontal plane is sweeping through 0^0, in order to minimize the wide band component of the beam.

This first horizontal bend string serves a dual purpose - it not only provides the momentum dispersion necessary for a dichromatic beam; in addition, because the first element of the string is so close to the production target, it also sweeps away low momentum secondaries and decreases this wide band beam component. Figure 5 shows the wide band rejection obtained in this design, when it is run at 600 GeV, in a

detector located in the vicinity of Lab C. Both right- and wrong-sign background are shown. Since the flux curves shown are for anti-neutrino running, they represent a "worst case" situation. The wide band background can be seen to be peaked at low energy, and is rapidly falling with increasing energy. Even at the lowest energy, the background is no worse than 10%, and within the design goal.

The dichromatic nature of the beam is shown in Figure 6a,b. Figure 6a shows the neutrino energy spectrum as a function of detector radius for the Lab C detector. The plot shown is for 750 GeV, the worst case. At any radius, the beam can be seen to separate into two bands, the lower energy band originating from pion decay, the higher energy band from kaon decay. Experiments exploit this energy-radius correlation, for example; neutral current physics, where the incoming neutrino energy can not be inferred from the measured interaction products. Figure 6b shows the radial separation between the two bands of neutrinos in a more quantitative way. This figure is for a 0.1m radial slice and demonstrates the pion/kaon neutrino separation is greater than 10^2.

The energy resolution of the beam is given in Figure 7a. This figure answers the question "How broad are the neutrino energy distributions in any given radial slice?". The design goal here was to have a resolution about 10% or less for radii up to one meter. For lower energy running, where the divergence of the beam is not so critical a factor,this design

goal is easily achieved. For 750 GeV, at first inspection, the energy resolution appears to be too large, climbing rapidly towards 20% at the higher radii. Figure 7b, however, shows that the actual number of events is falling as the radius increases. In addition, the energy of these neutrinos is also decreasing, so that when one combines these two effects, the average energy resolution, even out to a detector radius of 1.4m is about 11%.

In summary, the NCI design has met the stated design goals of high energy operation, clean proton dumping, small wide band background, good energy resolution, high flux and reduced cost. The angular acceptance achieved is well suited for high secondary energy running, but needs to be improved for lower energy tunes. How this will be accomplished is discussed in the next section.

Lower Energy Optimizations

As mentioned previously, one would like to keep the bend points fixed in order to minimize changes upstream of the target, but still introduce more quadrupoles for increased acceptance as the energy of the beam is lowered. Because the first bend string is composed of 4 magnets, there are then 3 discrete lower energy optimizations possible which can be built, at 3/4, 1/2 and 1/4 of 750 GeV. These individual designs are

called NCI562, NCI375 and NCI187 for the 562.5, 375 and 187.5 GeV geometries, respectively. As in the 750 GeV design, because we are trying to gather as much of the acceptance as possible, beam defining liners are necessary in the first two magnets. In the spirit of quick changeovers between the various energy designs, a concerted effort was made to keep the size of these liners consistent from design to design. Since all designs start with a bending magnet, its liner is the same as that of the 750 GeV design; 1.0" full width in height, and from -0.25" to +0.40" in width. The 375 and 187 GeV designs both have a 4Q120 quadrupole as the second magnet. The liner in this magnet for both designs was chosen to be 2.0" full width in height, and from -0.25" to +1.5" in width. The 562 GeV design has a 5-foot quadrupole as its second magnet. A liner of this same size should be sufficient in this quadrupole, however, this has not been studied in detail as of this report. (Although, from Figure 8, which shows proton beam dumping at 562, a width of -0.25" to +1.0" should also work.)

The three individual lower energy optimizations will be discussed in detail in the following sections.

NCI562 Optimization

The 562 GeV optimization requires 3 of the 4 bending magnets in the first dipole string. Because of this and the fact that we wish to retain the same bend points as the 750 GeV design, the NCI562 design requires two non-standard magnets. These are 5-foot quadrupoles, which fit in the two gaps between the 3 dipoles, and form the first element of a quadrupole triplet focus. The remaining two elements of the triplet are formed from the two 4Q120 quads and 4 of the 6 8NQ32A quads of the 750 GeV NCI beam. Of course, these latter quadrupoles have different positions than in the 750 GeV design, in order to cancel the momentum-dependent dispersive terms. Table A-2 details the beam element positions. Figure 8 shows how the primary proton beam will dump at both +562 and -562 GeV, the limiting cases for this geometry. For comparison, Figure 9 shows the increase in flux obtained with this design over that of the 750 GeV beam tuned to 562.5 GeV. Although at first glance, this may seem to be only a modest increase in flux, it should be pointed out that this curve is for the highest energy possible with this geometrical configuration. As will be discussed later, more substantial gains in flux over the 750 GeV beam are possible at lower ($375 < E < 562$ GeV) tunes.

NCI135 Optimization

The 375 GeV optimization is the one that has been the most extensively studied to date. Since this energy is 1/2 of 750 GeV, two of the first 4 dipoles can be replaced by quadrupoles for the first element of the triplet. As in the 562 GeV design, the remaining two triplet elements are formed from quadrupoles used in the 750 GeV beam; here, we use one of the 4Q120 quads (the second can be used for the second of the two front element quads, which does not require a liner) and 3 of the 6 8NQ32A quads. Table A-3 details the beam element positions. Figure 10 shows the proton beam dumping for both +375 and -375 GeV running, the limiting cases for this geometry. Shown on this figure for the two 4Q120 quads are two aperture sizes, the solid line outlining the vacuum chamber, and the dotted line indicating the good field region. Figure 11 shows the dichromatic nature of the NCI375 design, plotting the radial separation between the two bands of neutrinos, from pion and kaon decay. This figure is for a 0.1m radial slice, and shows that the level of separation is again about 10^2, as in the 750 GeV design. Finally Figure 12 compares the NCI375 design with that of the existing N30 dichromatic train, located in the target tube, set hypothetically to 375 GeV. Both beams give a comparable flux in the Lab C detector, with about equal resolution. To reiterate, more substantial gains in flux are possible with this geometry, as will be seen in a later example.

NCI187 Optimization

The final geometry considered is at 1/4 of 750 GeV, or 187.5 GeV. Here only one of the first four bending magnets is necessary, but in order to better reduce the wide band component of the beam, two dipoles were used, as in the 375 GeV design. As before, two 4Q120 quadrupoles are placed between them. To get the maximum acceptance, 4 of the 8NQ32A quadrupoles immediately follow this second dipole, to form a doublet focus. The remainder of the beam consists of bends centered about the 750 GeV bend points. Because of the doublet focus, the momentum-dependent dispersive terms of the matrix element can not be cancelled, but since this design is for a low energy, this is tolerable. Figure 13 shows the proton beam dumping. Again, the 4Q120 quadrupoles are shown with two apertures, as in Figure 10. It is clear from this figure that the last two 8NQ32A quadrupoles will have to be offset by an inch or so from beam center in order to avoid the proton beam, but this should cause no problem with the beam acceptance. This does imply that the bending magnets will have to run at a slightly different current to compensate for this effect, but it is not forseen as a difficulty. Beam element positions are given in Table A-4, which does not reflect these necessary offsets. Finally, Figure 14 shows a comparison between the NCI187 optimization and the existing N30 dichromatic train, located in the present target tube, at the usual Lab C detector. It can be seen from this figure that both beams have comparable resolution, but that the NCI187 design has about 30% or so more flux.

Other Intermediate Energy Tunes

As has been mentioned earlier, substantial gains in flux are possible over the limiting cases for the 562 and 375 GeV geometries. It was found that by running the first quadrupole element at the highest current possible at any given energy, and allowing the positions of the remaining two elements to vary in order to cancel the momentum-dependent dispersive terms, one obtained the maximum acceptance. This is not possible in the 750 GeV design nor in the 187 GeV optimization since these employ doublet focussing schemes. Figure 15 shows a t of vertical acceptance vs beam energy, with the horizontal acceptance at each of the points shown written below the beam energy axis. The four discrete beams are shown as circles on the figure, and a simple hand-drawn curve connects them. The triangle located at 275 GeV is the acceptance obtained using the above procedure, and is seen to agree well with the hand-drawn prediction.

Beam Monitoring

The level of beam monitoring equipment necessary for these designs is the same as that which exists today for the N30 dichromatic train. There are two hadron monitoring locations along the decay pipe; the expansion port and the target manhole. Located in both of these places are ion chambers to measure the total beam flux, and split-plate ion chambers used for beam steering. In addition, in the upsteam location; the expansion port, several other beam flux monitors exist, such as an RF cavity and a

beam toroid, as well as a Cerenkov counter to determine particle fractions. To see if the existing beam monitoring equipment will be useable with these new designs, several Monte Carlo calcula ns of beam sizes were carried out, both for the existing N30 train and for all of the new designs. The results are shown in Figures 16 and 17 a-d, respectively, which show beam sizes at the expansion port and the target manhole. The higher energy designs are easily contained within the existing ion chambers, and the lower energy designs, although larger, probably will also be contained. Ion chambers, because of new construction techniques, can be made better than existing equipment, and probably will be re-built for these Tevatron era beams[4].

Figure 18 shows a Cerenkov curve[5] obtained with the old D-61G design set at 600 GeV. Because of the new Front Hall location of these dichromatic beams, the possibility now exists to install the Cerenkov counter immediately downstream of the magnetic elements, thus insuring full containment of the beam. Studies are in progress on a new Cerenkov counter design, and preliminary work indicates that a new counter of 20 feet in length may be necessary for the higher energy running[4].

For muon monitoring, the large swics now under construction will be installed in the muon monitoring ports located in the berm.

Pre-targetting Transport

Enclosure G-2, located upstream of Front Hall is now thought of as a major switching area for conventional and prompt neutrino beams. Also located in this enclosure, shown in Figure 19, are 2 quadrupoles and 5 doubler dipoles which are pre-targetting elements for the new muon beam[6]. Upstream of G-2 in enclosures C and G-1, electrostatic septa and Lambertson magnets are located which split the muon and neutrino beams. In G-2 these beams are separated vertically. The doubler dipoles bend the muon transport off to the east at 30mr and away from the neutrino transport. This is the last enclosure that these two beams share in common.

Shown on the figure are 4 quadrupoles and 2 EPB dipoles for the neutrino transport. Current understanding of the Tevatron emittance leads to the conclusion that only 2 of these quads are sufficient in this location, however it can be seen that room does exist for additional elements should it prove necessary. These two dipoles provide a vertical switch for sending protons to a conventional beam, (such as the dichromatic beam described here, or a broad band beam[3]); or to the prompt neutrino facility[7], (which serves a dual purpose as a front end for calibration beams to the neutrino detectors). Either conventional neutrino beam can be served by this transport through G-2, since the targets are located at almost identical longitudinal and transverse locations. From G-2, the prompt beam follows the existing 400 GeV proton transport. The conventional neutrino beam is, of course, along a

different path, thus the pipe between G-2 and Front Hall must be modified. This is now scheduled to be completed during the summer of 1982 and is the last piece of construction necessary to provide 1 TeV operation of conventional neutrino beams in Front Hall.

Figures 20a and 20b show the layouts of Front Hall for a broad band triplet beam and for the 750 GeV NCI dichromatic beam, respectively. It can be seen from either of these figures that the prompt and conventional beams are now separated vertically. The lower beam to the prompt facility is made vertically flat and is bent to the east by a series of 7 rotated EPB dipoles. At the downstream end of the enclosure, it can be seen to be well separated from the conventional beams. It exits the hall via the final set of bends and quads shown on the drawings.

The top beam has the final elements of the pre-targetting transport, again using EPB quadrupoles to focus onto the production target. The dipoles shown, also EPB magnets, are either all vertical to level the beam for broad band targetting, or rotated at a constant angle to provide the proper combination of vertical and horizontal targetting angles and positions necessary for the dichromatic beam. Table A-5 gives the pre-target beam element positions for the NCI dichromatic target location, Table A-6 gives the pre-target beam element positions for a triplet target. Figure 21 shows schematically how either broad band or dichromatic pre-targetting can be accomplished using the same magnets

mounted on stands which they share with the prompt beam transport magnets. By employing rotations and small translations, either beam can be configured. Studies show that existing bedplates can be used here with modifications to the supporting structure. This pre-targetting area is then viewed as a permanent installation, with the flexibility to service a variety of physics programs.

References

1. L. Stutte, TM-841, "A Possible Dichromatic Beam for a 1 TeV Accelerator", January 1979.

2. A. Malensek, FN-341, "Empirical Formula for Thick Target Particle Production", October 1981.

3. S. Mori, TM-839, "Do We Need a Horn for Tevatron Neutrino Physics?", December 1978.

4. S. Pordes, private communication.

5. T. Kondo, private communication.

6. R. Evans, et al., TM-754, "Design Study for a High Energy Muon Beam", November 1977.

7. J. K. Walker, work in progress.

TABLE A-1 NCI BEAM POSITIONS 750 GeV

(Upstream and Downstream Ends of Magnets are Given)

ELEMENT	TYPE	FIELD(KG)	X(FT)	Y(FT)	Z(FT)	ROT(DEG)
TARGET			-1.1650	745.0425	3018.7500	
H BEND 1	6-3-120	-17.78488	-1.1711	745.0461	3019.7500	
			-1.2210	745.0823	3029.7498	
H BEND 2	6-3-120	-17.78488	-1.2289	745.0896	3031.7498	
			-1.2572	745.1258	3041.7496	
H BEND 3	6-3-120	-17.78488	-1.2607	745.1330	3043.7496	
			-1.2673	745.1692	3053.7496	
H BEND 4[1]	6-3-120	-17.78488	-1.2665	745.1764	3055.7495	
			-1.2514	745.2127	3065.7495	
NEGDUMP			-1.2463	745.2199	3067.7494	
			-1.2204	745.2561	3077.7494	
NEGDUMP			-1.2152	745.2633	3079.7493	
			-1.1893	745.2995	3089.7492	
POSDUMP			-1.1434	745.3638	3107.4991	
			-1.1176	745.4000	3117.4990	
POSDUMP			-1.1124	745.4072	3119.4989	
			-1.0865	745.4434	3129.4988	
H COLL			-1.0813	745.4507	3131.4988	
			-1.0555	745.4869	3141.4987	
HFQUAD 1	4Q120	4.32960	-1.0503	745.4941	3143.4987	
			-1.0244	745.5303	3153.4986	
HFQUAD 2	4Q120	4.32960	-1.0193	745.5376	3155.4986	
			-0.9934	745.5738	3165.4985	
V BEND 1	6-3-120	17.78488	-0.9882	745.5810	3167.4985	
			-0.9623	745.6064	3177.4984	
V BEND 2	6-3-120	17.78488	-0.9572	745.6093	3179.4984	
			-0.9313	745.6130	3189.4983	
V BEND 3	6-3-120	17.78488	-0.9261	745.6115	3191.4983	
			-0.9003	745.5936	3201.4983	

V BEND 4	6-3-120	17.78488	-0.8951	745.5878	3203.4983	
			-0.8692	745.5482	3213.4982	
V BEND 5	6-3-120	17.78488	-0.8640	745.5381	3215.4981	
			-0.8382	745.4768	3225.4979	
VFQUAD 1	8NQ32A	-2.91554	-0.8330	745.4623	3227.4978	
			-0.8252	745.4407	3230.4978	
VFQUAD 2	8NQ32A	-2.91554	-0.8201	745.4263	3232.4977	
			-0.8123	745.4046	3235.4976	
VFQUAD 3	8NQ32A	-2.91554	-0.8071	745.3902	3237.4976	
			-0.7994	745.3686	3240.4975	
VFQUAD 4	8NQ32A	-2.91554	-0.7942	745.3541	3242.4974	
			-0.7864	745.3325	3245.4973	
VFQUAD 5	8NQ32A	-2.91554	-0.7813	745.3181	3247.4973	
			-0.7735	745.2964	3250.4972	
VFQUAD 6	8NQ32A	-2.91554	-0.7683	745.2820	3252.4971	
			-0.7606	745.2604	3255.4970	
H COLL			-0.7554	745.2459	3257.4970	
			-0.7295	745.1738	3267.4967	
R BEND 1	6-3-120	15.72115	-0.7244	745.1594	3269.4966	70.24936
			-0.7017	745.0962	3279.4964	CCW
R BEND 2	6-3-120	15.72115	-0.6979	745.0854	3281.4964	70.24936
			-0.6817	745.0403	3291.4962	CCW
R BEND 3	6-3-120	15.72115	-0.6791	745.0331	3293.4962	70.24936
			-0.6694	745.0060	3303.4962	CCW
R BEND 4	6-3-120	15.72115	-0.6681	745.0024	3305.4962	70.24936
			-0.6649	744.9934	3315.4962	CCW

1. Additional offset of 2" East must be added (-0.1667).

TABLE A-2 NCI562 BEAM POSITIONS 562.5 GeV

(Upstream and Downstream Ends of Magnets are Given)

ELEMENT	TYPE	FIELD(KG)	X(FT)	Y(FT)	Z(FT)	ROT(DEG)
TARGET			-1.1650	745.0425	3018.7500	
H BEND 1	6-3-120	-17.78488	-1.1711	745.0461	3019.7500	
			-1.2174	745.0823	3029.7498	
VFQUAD 1	4Q60	-5.50	-1.2222	745.0878	3031.2498	
			-1.2382	745.1059	3036.2497	
H BEND 2	6-3-120	-17.78488	-1.2430	745.1113	3037.7497	
			-1.2604	745.1475	3047.7496	
VFQUAD 2	4Q60	-5.50	-1.2609	745.1529	3049.2496	
			-1.2624	745.1710	3054.2496	
H BEND 3[1]	6-3-120	-17.78488	-1.2628	745.1764	3055.7496	
			-1.2514	745.2127	3065.7495	
NEGDUMP			-1.2463	745.2199	3067.7495	
			-1.2204	745.2561	3077.7494	
NEGDUMP			-1.2152	745.2633	3079.7494	
			-1.1893	745.2995	3089.7493	
POSDUMP			-1.1786	745.3145	3093.8954	
			-1.1527	745.3507	3103.8953	
POSDUMP			-1.1476	745.3580	3105.8953	
			-1.1217	745.3942	3115.8952	
H COLL			-1.1165	745.4014	3117.8951	
			-1.0907	745.4376	3127.8950	
HFQUAD 1	4Q120	3.37867	-1.0855	745.4449	3129.8950	
			-1.0596	745.4811	3139.8949	
HFQUAD 2	4Q120	3.37867	-1.0544	745.4883	3141.8949	
			-1.0286	745.5245	3151.8948	
V BEND 1	6-3-120	16.67333	-0.9727	745.6027	3173.4984	
			-0.9468	745.6254	3183.4984	
V BEND 2	6-3-120	16.67333	-0.9416	745.6272	3185.4984	
			-0.9158	745.6228	3195.4983	

V BEND 3	6-3-120	16.67333	-0.9106	745.6192	3197.4983	
			-0.8847	745.5877	3207.4982	
V BEND 4	6-3-120	16.67333	-0.8796	745.5786	3209.4982	
			-0.8537	745.5201	3219.4980	
VFQUAD 1	8NQ32A	-2.85457	-0.8043	745.3824	3238.5804	
			-0.7966	745.3608	3241.5803	
VFQUAD 2	8NQ32A	-2.85457	-0.7914	745.3463	3243.5802	
			-0.7836	745.3247	3246.5802	
VFQUAD 3	8NQ32A	-2.85457	-0.7785	745.3103	3248.5801	
			-0.7707	745.2886	3251.5800	
VFQUAD 4	8NQ32A	-2.85457	-0.7655	745.2742	3253.5799	
			-0.7578	745.2525	3256.5799	
H COLL			-0.7399	745.2026	3263.4967	
			-0.7140	745.1305	3273.4964	
R BEND 1	6-3-120	15.72115	-0.7089	745.1161	3275.4963	70.24936
			-0.6873	745.0560	3285.4961	CCW
R BEND 2	6-3-120	15.72115	-0.6839	745.0463	3287.4961	70.24936
			-0.6709	745.0103	3297.4960	CCW
R BEND 3	6-3-120	15.72115	-0.6692	745.0054	3299.4960	70.24936
			-0.6649	744.9934	3309.4960	CCW

1. Additional offset of 1.5" East must be added (-0.1250).

TABLE A-3 NCI375 BEAM POSITIONS 375 GeV

(Upstream and Downstream Ends of Magnets are Given)

ELEMENT	TYPE	FIELD(KG)	X(FT)	Y(FT)	Z(FT)	ROT(DEG)
TARGET			-1.1650	745.0425	3018.7500	
H BEND 1	6-3-120	-17.78488	-1.1711	745.0461	3019.7500	
			-1.2102	745.0823	3029.7498	
VFQUAD 1	4Q120	-5.50	-1.2137	745.0896	3031.7498	
			-1.2312	745.1258	3041.7497	
VFQUAD 2	4Q120	-5.50	-1.2347	745.1330	3043.7497	
			-1.2521	745.1692	3053.7496	
H BEND 2[1]	6-3-120	-17.78488	-1.2556	745.1764	3055.7496	
			-1.2514	745.2127	3065.7495	
NEGDUMP			-1.2463	745.2199	3067.7495	
			-1.2204	745.2561	3077.7494	
NEGDUMP			-1.2152	745.2633	3079.7494	
			-1.1893	745.2995	3089.7493	
POSDUMP			-1.1976	745.2880	3086.5704	
			-1.1717	745.3242	3096.5703	
POSDUMP			-1.1665	745.3315	3098.5703	
			-1.1407	745.3677	3108.5702	
H COLL			-1.1355	745.3749	3110.5701	
			-1.1096	745.4111	3120.5700	
HFQUAD 1	4Q120	4.77478	-1.1044	745.4183	3122.5700	
			-1.0786	745.4546	3132.5699	
V BEND 1	6-3-120	14.82073	-0.9572	745.6244	3179.4984	
			-0.9313	745.6426	3189.4984	
V BEND 2	6-3-120	14.82073	-0.9261	745.6426	3191.4984	
			-0.9003	745.6246	3201.4983	
V BEND 3	6-3-120	14.82073	-0.8951	745.6174	3203.4983	
			-0.8692	745.5633	3213.4981	
VFQUAD 1	8NQ32A	-2.16632	-0.7763	745.3042	3249.4233	
			-0.7685	745.2825	3252.4232	

VFQUAD 2	8NQ32A	-2.16632	-0.7634	745.2681	3254.4231	
			-0.7556	745.2465	3257.4230	
VFQUAD 3	8NQ32A	-2.16632	-0.7504	745.2320	3259.4230	
			-0.7427	745.2104	3262.4229	
H COLL			-0.7244	745.1594	3269.4964	
			-0.6985	745.0872	3279.4962	
R BEND 1	6-3-120	15.72115	-0.6933	745.0728	3281.4961	70.24936
			-0.6739	745.0187	3291.4959	CCW
R BEND 2	6-3-120	15.72115	-0.6714	745.0115	3293.4959	70.24936
			-0.6649	744.9934	3303.4959	CCW

1. Additional offset of 1" East must be added (-0.0833).

TABLE A-4 NCI187 BEAM POSITIONS 187.5 GeV

(Upstream and Downstream Ends of Magnets are Given)

ELEMENT	TYPE	FIELD(KG)	X(FT)	Y(FT)	Z(FT)	ROT(DEG)
TARGET			-1.1650	745.0425	3018.7500	
H BEND 1	6-3-120	-8.89244	-1.1711	745.0461	3019.7500	
			-1.2102	745.0823	3029.7498	
VFQUAD 1	4Q120	-6.05354	-1.2137	745.0896	3031.7498	
			-1.2312	745.1258	3041.7497	
VFQUAD 2	4Q120	-6.05354	-1.2347	745.1330	3043.7497	
			-1.2521	745.1692	3053.7496	
H BEND 2	6-3-120	-8.89244	-1.2556	745.1764	3055.7496	
			-1.2514	745.2127	3065.7495	
HFQUAD 1	8NQ32A	3.84731	-1.2463	745.2199	3067.7495	
			-1.2385	745.2308	3070.7495	
HFQUAD 2	8NQ32A	3.84731	-1.2333	745.2380	3072.7495	
			-1.2256	745.2489	3075.7494	
HFQUAD 3[1]	8NQ32A	3.84731	-1.2204	745.2561	3077.7494	
			-1.2126	745.2670	3080.7494	
HFQUAD 4[2]	8NQ32A	3.84731	-1.2075	745.2742	3082.7494	
			-1.1997	745.2851	3085.7493	
DUMP			-1.1945	745.2923	3087.7493	
			-1.1686	745.3285	3097.7492	
DUMP			-1.1635	745.3357	3099.7492	
			-1.1376	745.3719	3109.7491	
V COLL			-0.9727	745.6027	3173.4985	
			-0.9468	745.6389	3183.4984	
V BEND 1	6-3-120	11.11555	-0.9416	745.6461	3185.4984	
			-0.9158	745.6553	3195.4983	
V BEND 2	6-3-120	11.11555	-0.9106	745.6517	3197.4983	
			-0.8847	745.6066	3207.4981	
V COLL			-0.7089	745.1161	3275.4962	
			-0.6830	745.0439	3285.4959	

R BEND 1	6-3-120	15.72115	-0.6778	745.0296	3287.4958	70.24936
			-0.6649	744.9935	3297.4957	CCW

1. Additional offset of 1" East must be added (-0.0833).

2. Additional offset of 2" East must be added (-0.1667).

TABLE A-5 PROTON BEAM TRANSPORT 1000 GeV

TO NCI 750 GeV TARGET

(Upstream and Downstream Ends of Magnets are Given)

ELEMENT	TYPE	FIELD(KG)	X(FT)	Y(FT)	Z(FT)	ROT(DEG)
			Enclosure G-2 Magnets			
VFQ120 1	EPBQUAD	-3.01884	-0.6699	735.5699	2227.4450	
			-0.6699	735.6708	2237.4445	
VFQ120 2	EPBQUAD	-3.01884	-0.6699	735.6808	2238.4445	
			-0.6699	735.7817	2248.4440	
HFQ120 1	EPBQUAD	2.53347	-0.6699	735.9935	2269.4429	
			-0.6699	736.0943	2279.4424	
HFQ120 2	EPBQUAD	2.53347	-0.6699	736.1044	2280.4423	
			-0.6699	736.2052	2290.4418	
RB VG2 1	EPBBEND	-17.11627	-0.6699	736.2153	2291.4418	90.56380
			-0.6700	736.3240	2301.4412	CW
RB VG2 2	EPBBEND	-17.11627	-0.6700	736.3356	2302.4411	90.56380
			-0.6702	736.4599	2312.4403	CW
H BEND 1	TRIM	-0.00010	-0.6714	736.9554	2349.9371	
			-0.6714	736.9884	2352.4368	
			Front Hall Magnets			
H BEND 2	TRIM	-0.00001	-0.6871	743.7477	2863.9802	
			-0.6872	743.7807	2866.4800	
HF FG3 1	EPBQUAD	4.62641	-0.6873	743.8005	2867.9799	
			-0.6876	743.9327	2877.9790	
HF FG3 2	EPBQUAD	4.62641	-0.6876	743.9459	2878.9789	
			-0.6879	744.0780	2888.9780	
RB VG3 1	EPBBEND	17.72983	-0.6879	744.0912	2889.9779	57.76026
			-0.6926	744.2165	2899.9772	CW
RB VG3 2	EPBBEND	17.72983	-0.6934	744.2283	2900.9771	57.76026
			-0.7067	744.3399	2910.9765	CW

RB VG3 3	EPBBEND	17.72983	-0.7085	744.3504	2911.9764	57.76026
			-0.7304	744.4482	2921.9759	CW
RB VG3 4	EPBBEND	17.72983	-0.7330	744.4573	2922.9758	57.76026
			-0.7636	744.5415	2932.9754	CW
RB VG3 5	EPBBEND	17.72983	-0.7671	744.5492	2933.9754	57.76026
			-0.8063	744.6197	2943.9751	CW
VF DG3 1	EPBQUAD	-5.60577	-0.8106	744.6260	2944.9751	
			-0.8541	744.6897	2954.9748	
VF DG3 2	EPBQUAD	-5.60577	-0.8585	744.6960	2955.9747	
			-0.9020	744.7596	2965.9744	
VF DG3 3	EPBQUAD	-5.60577	-0.9064	744.7660	2966.9744	
			-0.9499	744.8296	2976.9741	
VF DG3 4	EPBQUAD	-5.60577	-0.9542	744.8360	2977.9741	
			-0.9977	744.8996	2987.9738	
RB VG3 6	EPBBEND	17.72983	-1.0021	744.9059	2988.9737	57.76026
			-1.0499	744.9627	2998.9735	CW
RB VG3 7	EPBBEND	17.72983	-1.0551	744.9677	2999.9734	57.76026
			-1.1116	745.0107	3009.9732	CW
TARGET			-1.1650	745.0425	3018.7500	

TABLE A-6 PROTON BEAM TRANSPORT 1000 GeV

TO TRIPLET TARGET

(Upstream and Downstream Ends of Magnets are Given)

ELEMENT	TYPE	FIELD(KG)	X(FT)	Y(FT)	Z(FT)	ROT(DEG)
			Enclosure G-2 Magnets			
VFQ120 1	EPBQUAD	-2.98010	-0.6699	735.5699	2227.4450	
			-0.6699	735.6708	2237.4445	
VFQ120 2	EPBQUAD	-2.98010	-0.6699	735.6808	2238.4445	
			-0.6699	735.7817	2248.4440	
HFQ120 1	EPBQUAD	2.57909	-0.6699	735.9935	2269.4429	
			-0.6699	736.0943	2279.4424	
HFQ120 2	EPBQUAD	2.57909	-0.6699	736.1044	2280.4423	
			-0.6699	736.2052	2290.4418	
RB VG2 1	EPBBEND	-17.14051	-0.6699	736.2153	2291.4418	90.00000
			-0.6699	736.3240	2301.4412	CW
RB VG2 2	EPBBEND	-17.14051	-0.6699	736.3357	2302.4411	90.00000
			-0.6699	736.4600	2312.4403	CW
H BEND 1	TRIM	0.01479	-0.6699	736.9556	2349.9371	
			-0.6699	736.9887	2352.4368	
			Front Hall Magnets			
H BEND 2	TRIM	-0.01045	-0.6700	743.7503	2863.9802	
			-0.6700	743.7833	2866.4800	
HF FG3 1	EPBQUAD	4.37731	-0.6700	743.8031	2867.9798	
			-0.6700	743.9353	2877.9790	
HF FG3 2	EPBQUAD	4.37731	-0.6700	743.9485	2878.9789	
			-0.6700	744.0807	2888.9780	
RB VG3 1	EPBBEND	16.07171	-0.6700	744.0939	2889.9779	90.00000
			-0.6700	744.2187	2899.9771	CW
RB VG3 2	EPBBEND	16.07171	-0.6700	744.2305	2900.9771	90.00000
			-0.6700	744.3406	2910.9765	CW

RB VG3 3	EPBBEND	16.07171	-0.6700	744.3509	2911.9764	90.00000
			-0.6700	744.4463	2921.9759	CW
RB VG3 4	EPBBEND	16.07171	-0.6700	744.4552	2922.9759	90.00000
			-0.6700	744.5359	2932.9756	CW
RB VG3 5	EPBBEND	16.07171	-0.6700	744.5433	2933.9756	90.00000
			-0.6700	744.6094	2943.9753	CW
VF DG3 1	EPBQUAD	-4.90076	-0.6700	744.6152	2944.9753	
			-0.6700	744.6740	2954.9751	
VF DG3 2	EPBQUAD	-4.90076	-0.6700	744.6799	2955.9751	
			-0.6700	744.7386	2965.9750	
VF DG3 3	EPBQUAD	-4.90076	-0.6700	744.7445	2966.9749	
			-0.6700	744.8032	2976.9748	
VF DG3 4	EPBQUAD	-4.90076	-0.6700	744.8091	2977.9747	
			-0.6700	744.8678	2987.9746	
RB VG3 6	EPBBEND	16.07171	-0.6700	744.8737	2988.9746	90.00000
			-0.6700	744.9251	2998.9744	CW
RB VG3 7	EPBBEND	16.07171	-0.6700	744.9295	2999.9744	90.00000
			-0.6700	744.9662	3009.9743	CW
RB VG3 8	EPBBEND	16.07171	-0.6700	744.9692	3010.9743	90.00000
			-0.6700	744.9912	3020.9743	CW
RB VG3 9	EPBBEND	16.07171	-0.6700	744.9927	3021.9743	90.00000
			-0.6700	745.0000	3031.9743	CW
H BEND 1	TRIM	-0.00046	-0.6700	745.0000	3032.9743	
			-0.6700	745.0000	3035.4743	
TARGET			-0.6700	745.0000	3037.0000	

Figure Captions

1. Number of events/ 10^{13} protons in the Lab E detector, for neutrino and anti-neutrino running, with either 400 GeV or 1 TeV protons incident on a production target. The beam is assumed to have an acceptance at all momenta comparable to that achieved in the existing N30 train.

2. The percentage of flux in either plane within a given production angle for a 10% momentum bite, assuming 1 TeV incident on a production target. Taken from Reference 2.

3. Conceptual layout for the 750 GeV NCI dichromatic beam. The upper part of the figure shows the vertical plane, the lower part of the figure shows the horizontal plane. Bend angles are as indicated.

4. Proton beam dumping for the 750 GeV NCI beam. Shown are the trajectories taken by the non-interacting primary proton beam for both +750 and -750 GeV operation, the limiting cases; and also for 600 GeV operation. In addition the beam envelope is indicated. Liners inserted into magnet apertures are indicated in cross-hatching, as are beam dumps. Dump positions are indicated for both positive and negative running; the same dumps will be used and moved into the appropriate locations. Two apertures are shown for the 4Q120 quadrupoles. The solid line indicates the vacuum jacket and the dotted line indicates the good field region.

5. Anti-neutrino flux spectra seen at a detector located at the z position of Lab C, with a one meter radius. Shown are the anti-neutrino flux, and wide-band backgrounds of both sign.

6. (a) Neutrino energy spectrum as a function of detector radius, for the Lab C detector. NCI beam tuned to 750 GeV. (b) A radial slice of the above plot, for radii from 0.6 - 0.7 m.

7. (a) Energy resolution for the NCI beam (750 GeV version) when tuned to several different momenta as a function of detector radius, observed in Lab C. (b) For the 750 GeV tune, the number of events and the energy spectrum of these events, as a function of detector radius.

8. Primary proton beam dumping for the NCI562 optimization. Shown are the primary proton beam trajectories for +562 and -562 GeV tunes, the limiting cases, and the beam envelope. Two apertures are drawn for the 4Q120 quadrupoles, the solid line for the vacuum jacket, and the dotted line for the good-field region. Shown in cross-hatch are magnet liners and beam dumps. Dump positions are indicated for both positive and negative running; the same dumps will be used and moved into the appropriate locations.

9. Neutrino flux for the NCI562 and the NCI beams, tuned to 562.5 GeV, in the Lab C detector, 1 m radius.

10. Primary proton beam dumping for the NCI375 optimization. Shown are the primary proton beam trajectories for +375 and -375 GeV tunes, the limiting cases, and the beam envelope. 4Q120 quadrupole apertures as in figure 8. Liners and beam dumps shown in cross-hatching. Dump positions are indicated for both positive and negative running; the same dumps will be used and moved into the appropriate locations.

11. A radial slice of the neutrino energy spectrum, for the NCI375 optimization, for radii between 0.5 and 0.6m.

12. Neutrino flux for the NCI375 optimization and the existing N30 dichromatic train, hypothetically tuned to 375 GeV, in the Lab C detector, 1 m radius.

13. Primary proton beam dumping for the NCI187 optimization. Shown are the proton beam trajectories for +187 and -187 GeV tunes, the limiting cases, and the beam envelope. 4Q120 quadrupole apertures as in Figure 8. Liners and beam dumps shown in cross-hatching. A single beam dump location serves for both positive and negative running.

14. Neutrino flux curves for the NCI187 optimization and the existing N30 train tuned to 187.5 GeV, in the Lab C detector, 1 m radius.

15. Acceptance in the vertical plane for various NCI optimizations (circles) versus beam energy. The horizontal plane acceptances are indicated on the figure under the appropriate position. The

triangle shows the acceptance attained at an intermediate energy of 275 GeV, using the 375 GeV geometry.

16. Beam profiles for the existing N30 dichromatic train at the expansion port and the target manhole monitoring stations.

17. Beam profiles for the NCI beam designs at the expansion port and the target manhole monitoring stations. (a) NCI 750 GeV, (b) NCI562, (c) NCI375, (d) NCI187.

18. Cerenkov curve for the D-61G dichromatic train tuned to 600 GeV, described in reference 1. Plot is due to T. Kondo.

19. Layout of Enclosure G-2, showing the proton transport for the 1 TeV muon beam, described in reference 6, and the proton transport for the conventional neutrino program; e. g. this dichromatic beam design and wide band beams described in reference 3.

20. (a) Layout for Front Hall showing a wide band beam and the prompt transport. (b) Layout for Front Hall showing the 750 GeV NCI beam and the prompt transport.

21. Schematic showing the mounting for the pre-targetting magnets for either of the conventional neutrino beams (wide band beam is shown level, NCI dichromatic beam is shown at an angle) and the prompt transport.

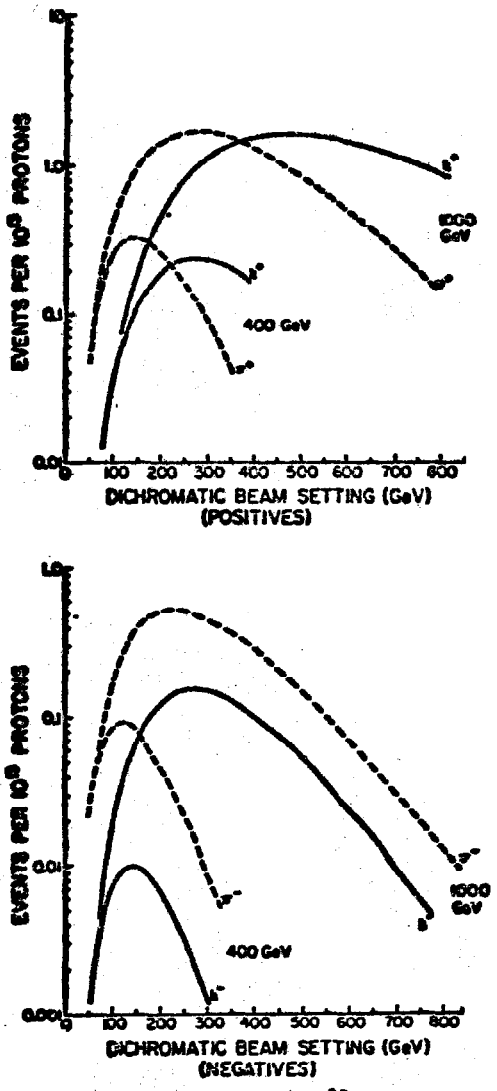

Figure 10: Events per 10^{13} protons vs. dichromatic beam setting. The top (bottom) plot is for neutrino (antineutrino) events with two sets of curves for 400 GeV and 1000 GeV incident protons.

FIGURE 1

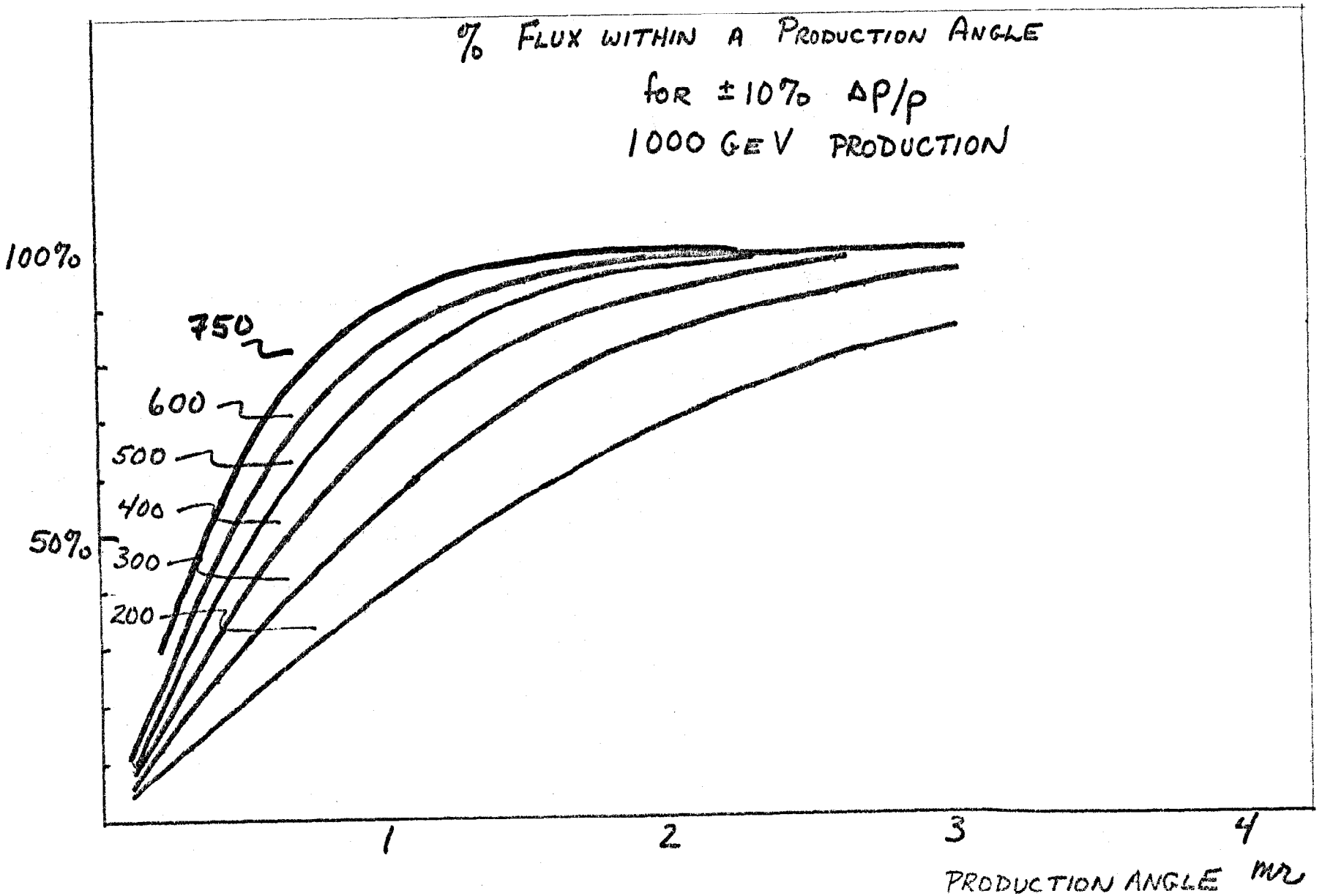
% FLUX WITHIN A PRODUCTION ANGLE
FOR ±10% ΔP/P
1000 GEV PRODUCTION
100%
50%
750
600
500
400
300
200
1
2
3
4
PRODUCTION ANGLE mr

FIGURE 2

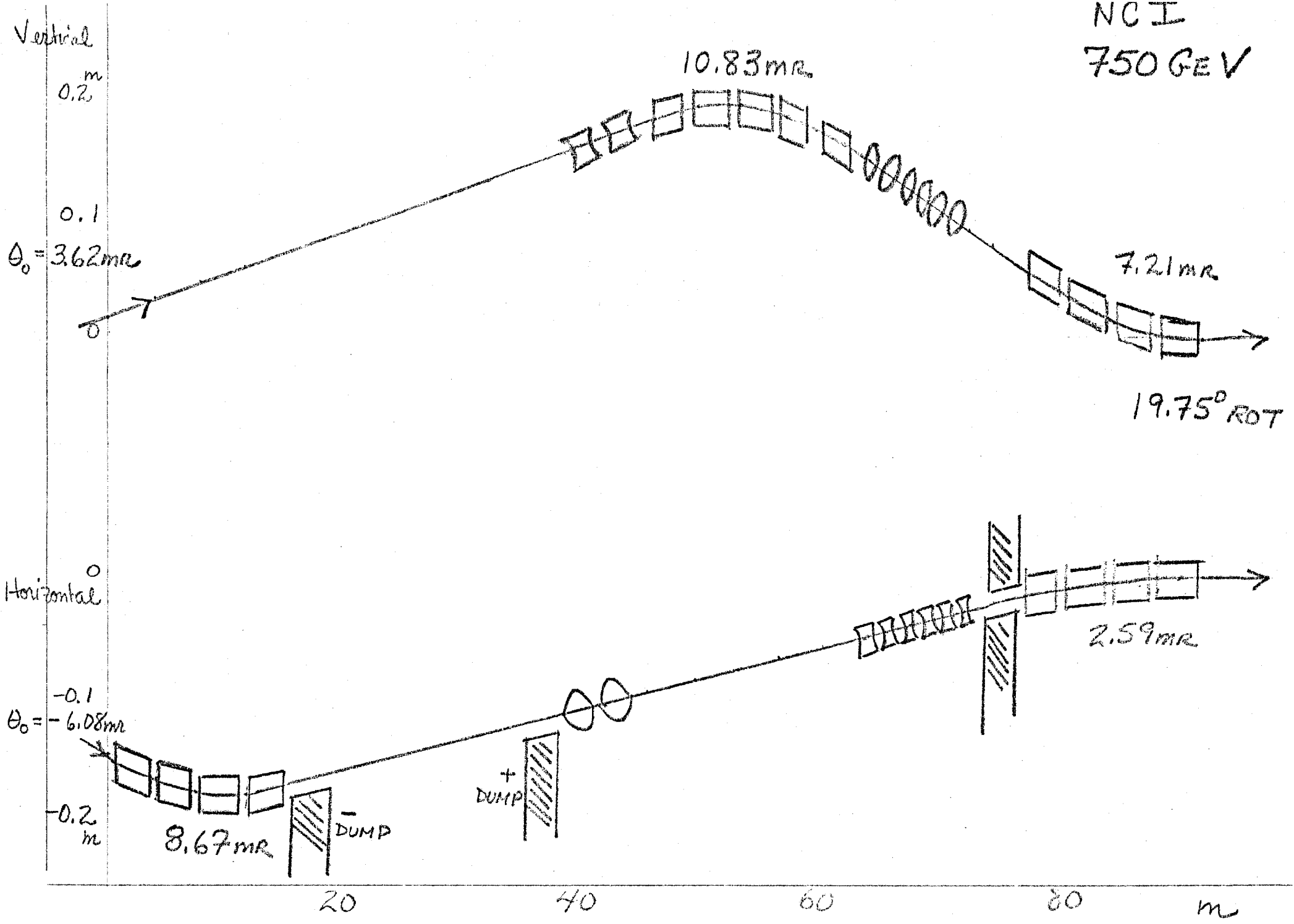
NCI
750 GEV
Vertical
m
0.2
0.1
θ_0 = 3.62mR
0
10.83mR
7.21mR
19.75° ROT
Horizontal
0
-0.1
θ_0 = - 6.08mR
-0.2
m
8.67mR
DUMP
+
DUMP
2.59mR
20
40
60
80
m

FIGURE 3

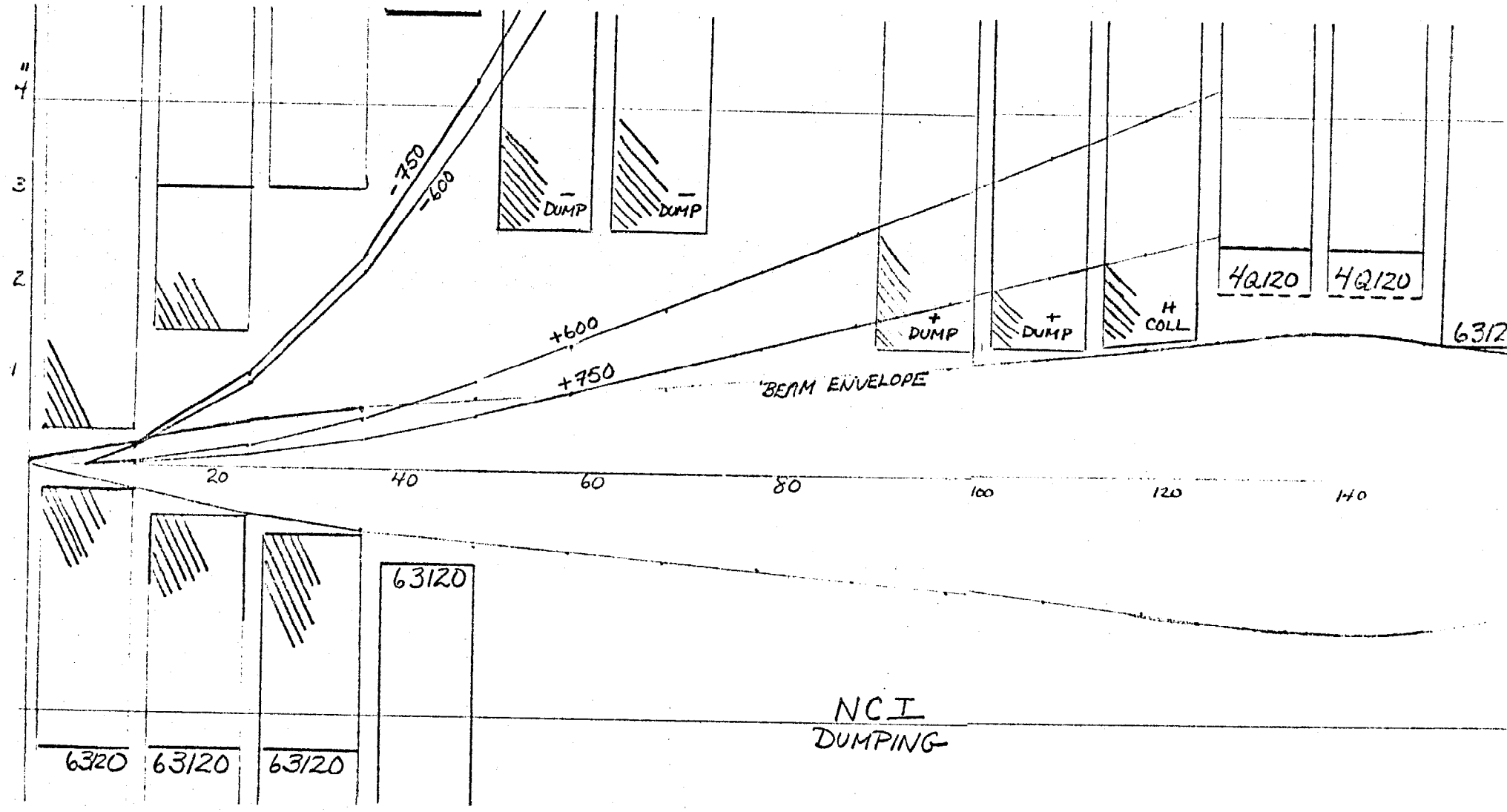
4"
3
2
1
-750
-600
DUMP
DUMP
+600
+750
BEAM ENVELOPE
+
DUMP
+
DUMP
H
COLL
4Q120
4Q120
6312
20
40
60
80
100
120
140
63120
63120
63120
63120
NCI
DUMPING

FIGURE 4

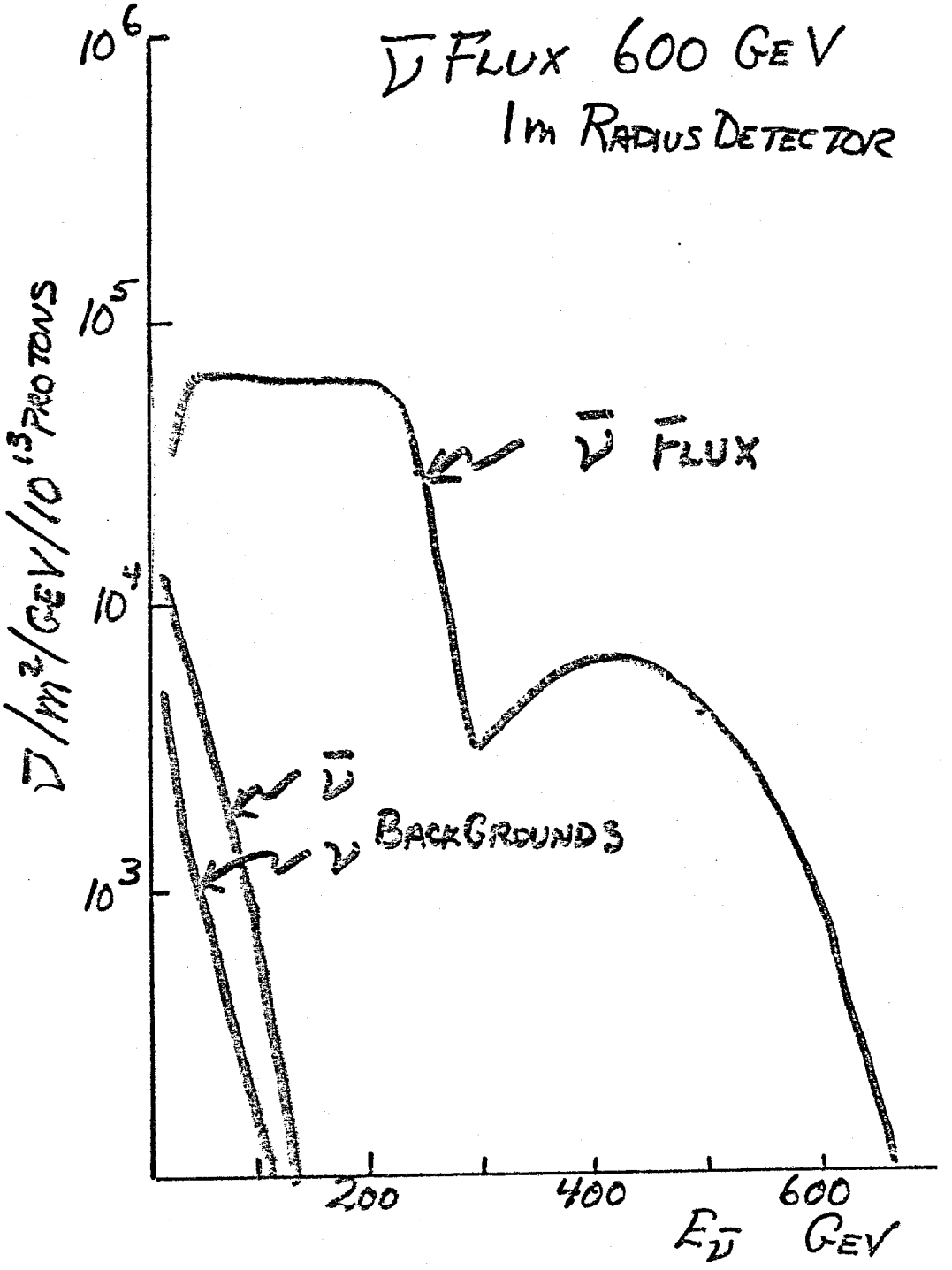
$\bar{\nu}$ FLUX 600 GEV
1m RADIUS DETECTOR
10^6
10^5
10^4
10^3
$\bar{\nu}$ FLUX
$\bar{\nu}$
ν BACKGROUNDS
200
400
600
$E_{\bar{\nu}}$ GEV

FIGURE 5

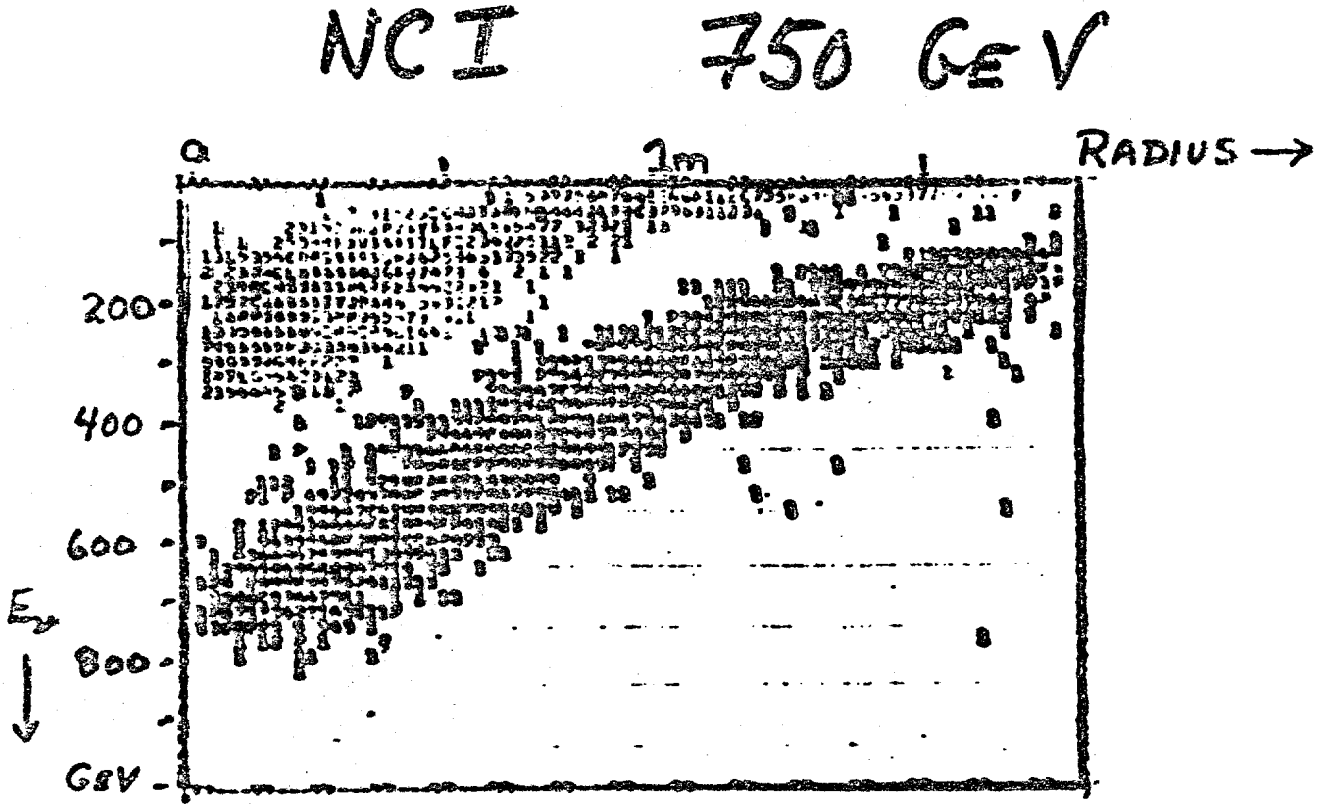

FIGURE 6A

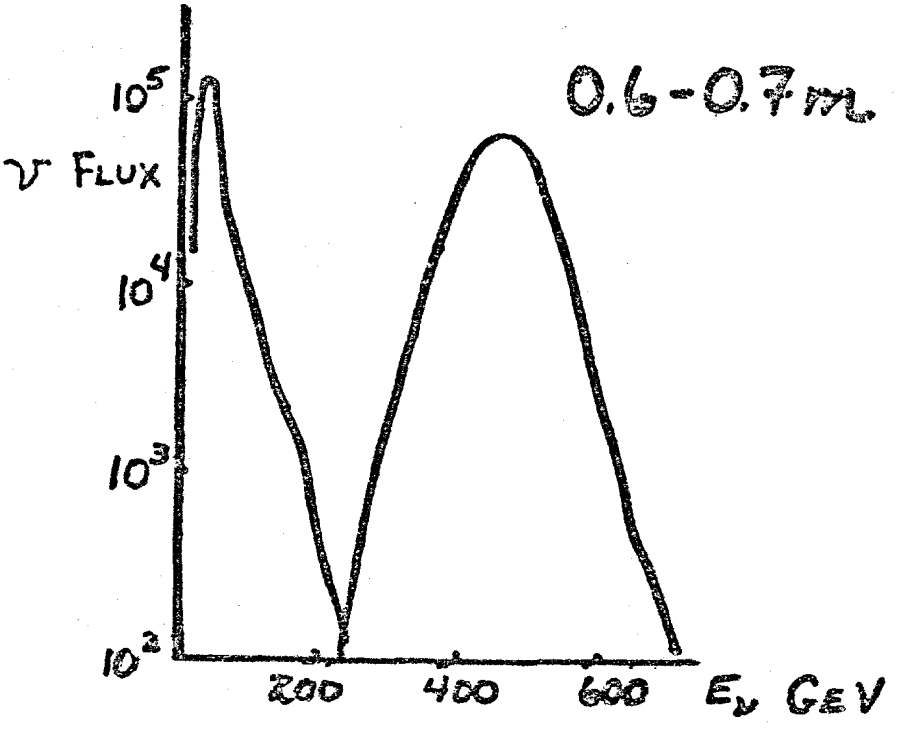

FIGURE 6B

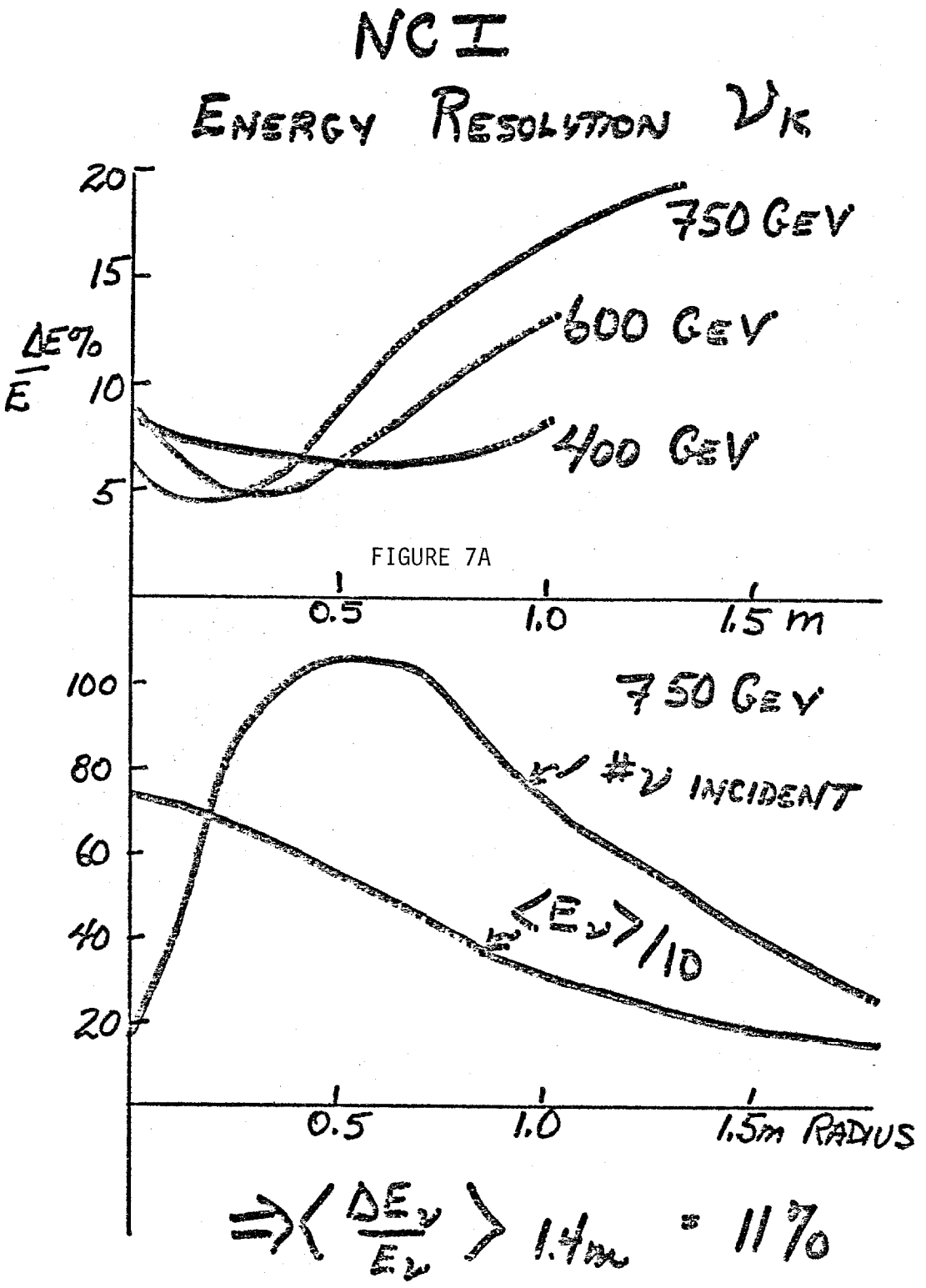

FIGURE 7A

FIGURE 7B

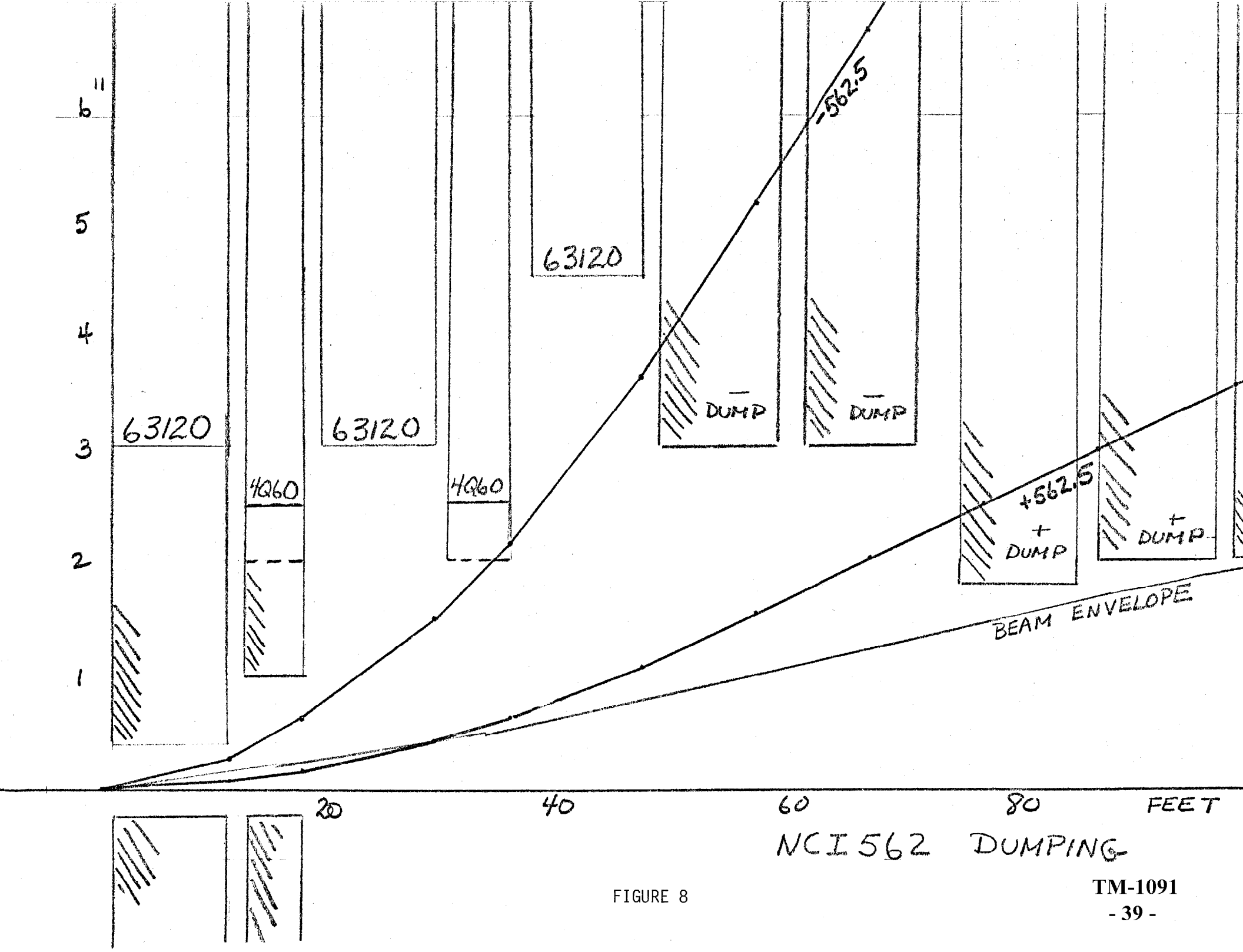
6"
5
4
3
2
1
63120
4Q60
63120
4Q60
63120
DUMP
DUMP
-562.5
+562.5
+
DUMP
+
DUMP
BEAM ENVELOPE
20
40
60
80
FEET
NCI562 DUMPING

FIGURE 8

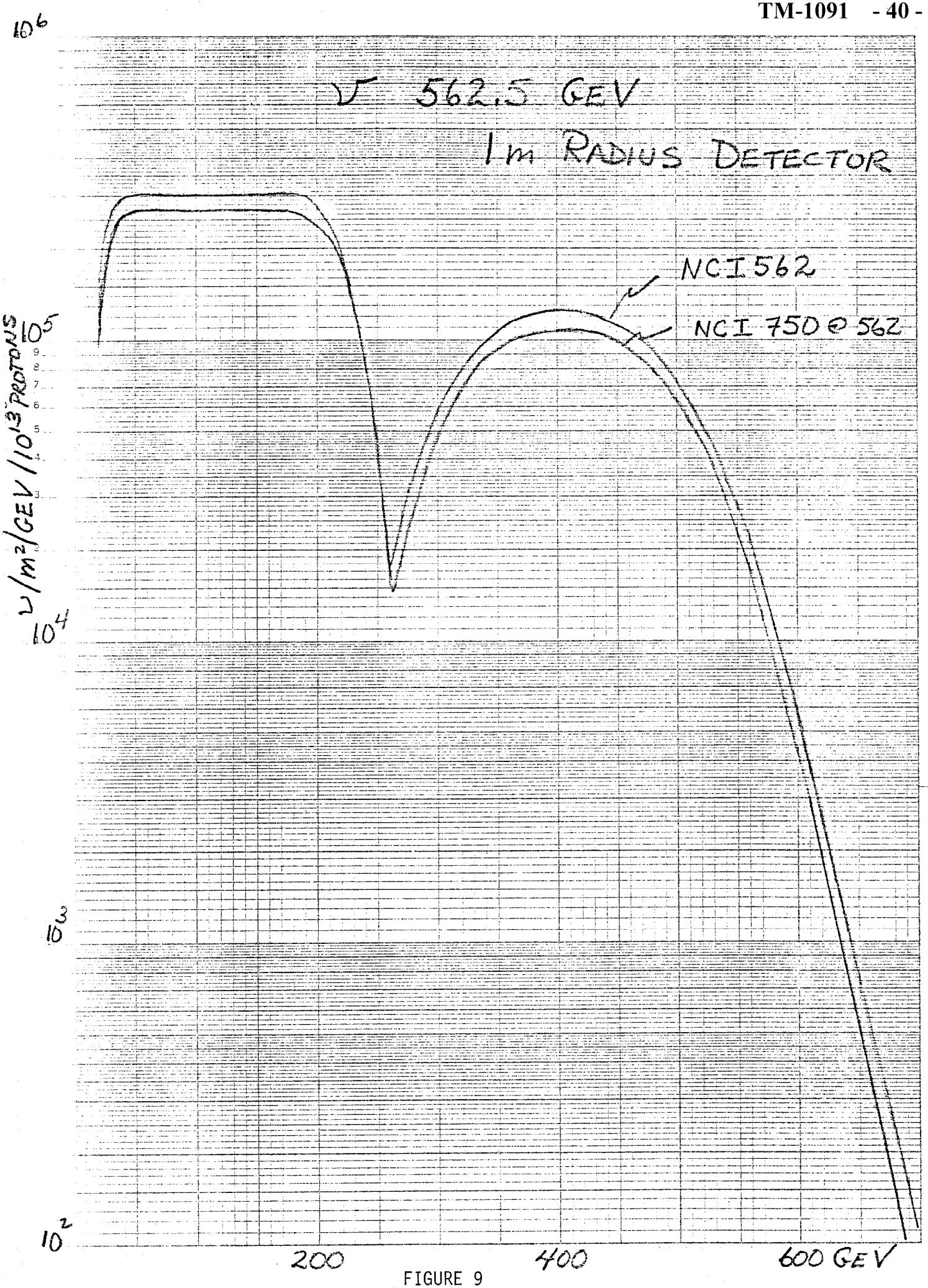
$\sqrt{s}$ 562.5 GEV
1m RADIUS DETECTOR
NCI562
NCI 750 @ 562
10^6
10^5
10^4
10^3
10^2
$\nu/m^2/GEV/10^{13}$ PROTONS
200
400
600 GEV

FIGURE 9

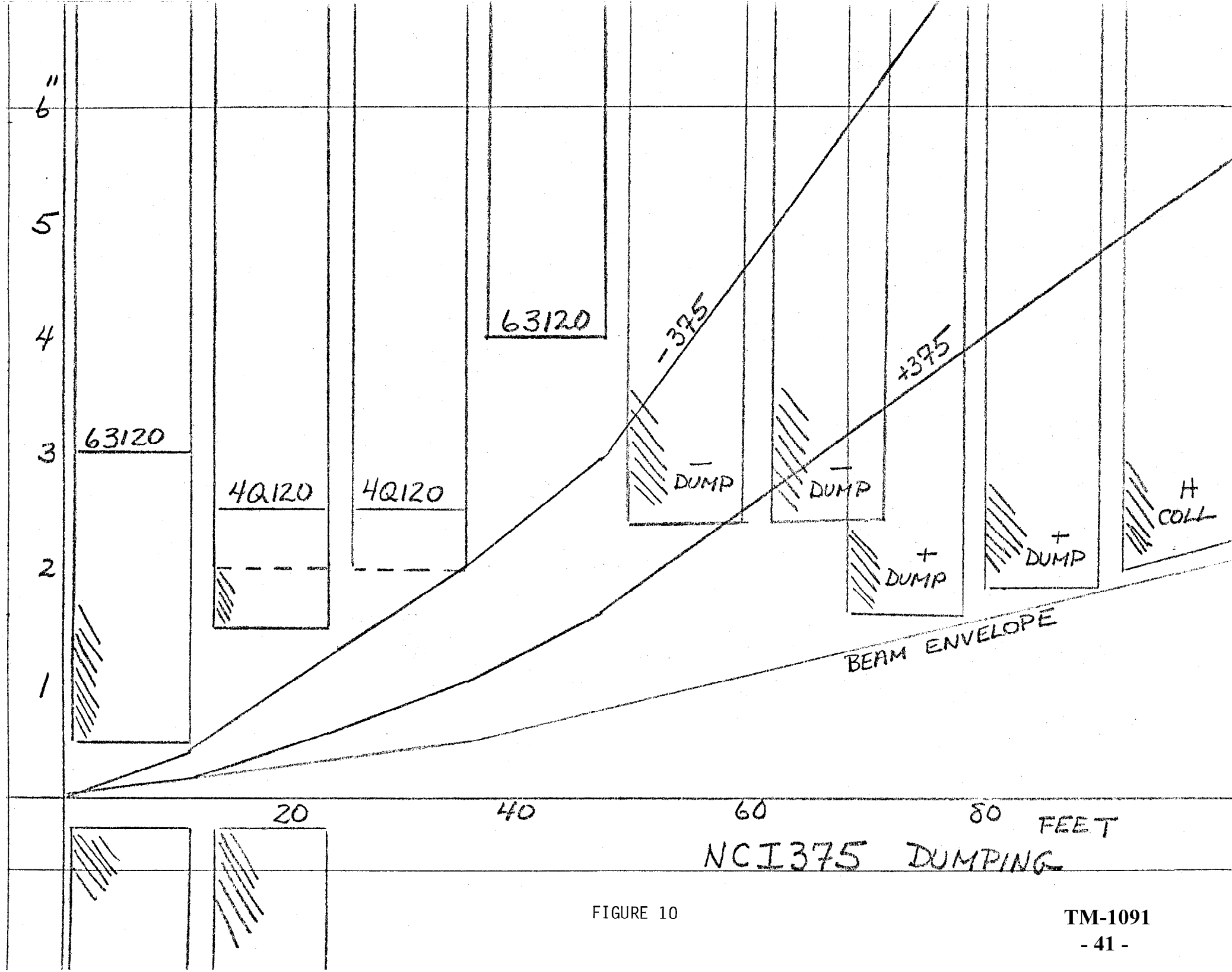
6"
5
4
3
2
1
63120
4Q120
4Q120
63120
-375
+375
DUMP
DUMP
+
DUMP
+
DUMP
H
COLL
BEAM ENVELOPE
20
40
60
80
FEET
NCI375 DUMPING

FIGURE 10

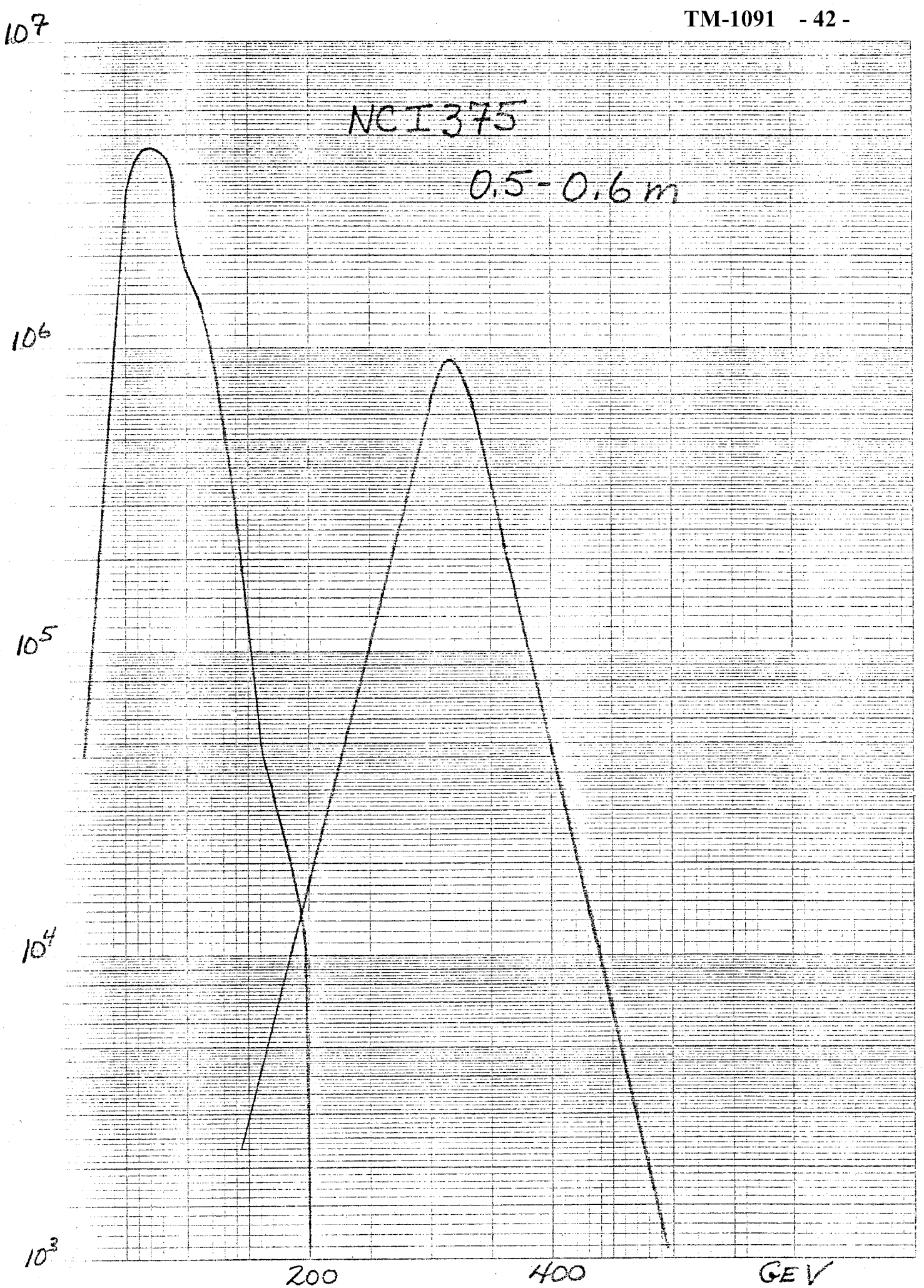

FIGURE 11

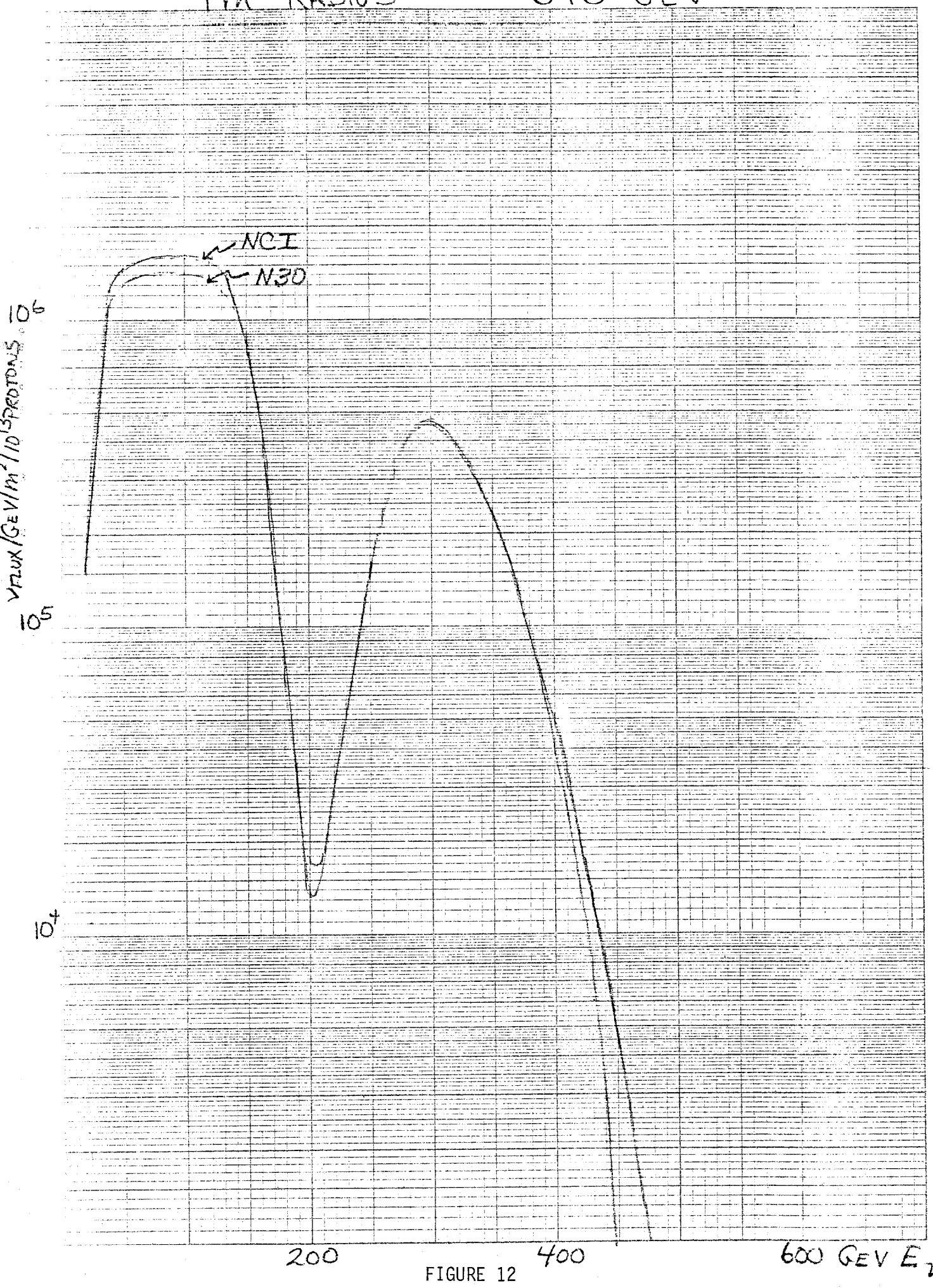
1m RADIUS
375 GeV
NC1
N30
10^6
10^5
10^4
ν_{FLUX}/GeV/m^2/10^{13}PROTONS
200
400
600 GeV E_ν

FIGURE 12

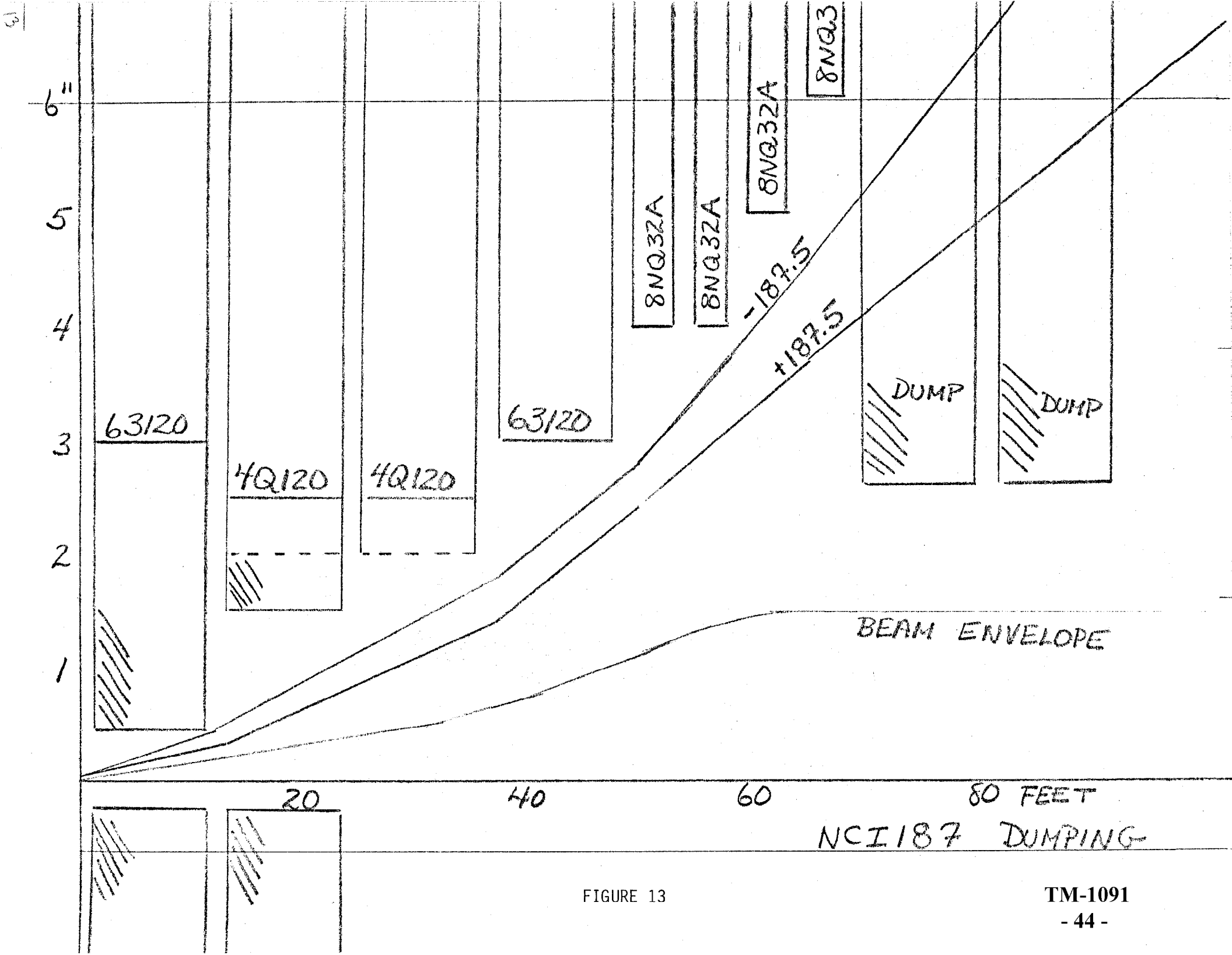
6"
5
4
3
2
1
63120
4Q120
4Q120
63120
8NQ32A
8NQ32A
8NQ32A
8NQ3
-187.5
+187.5
DUMP
DUMP
BEAM ENVELOPE
20
40
60
80 FEET
NCI187 DUMPING-

FIGURE 13

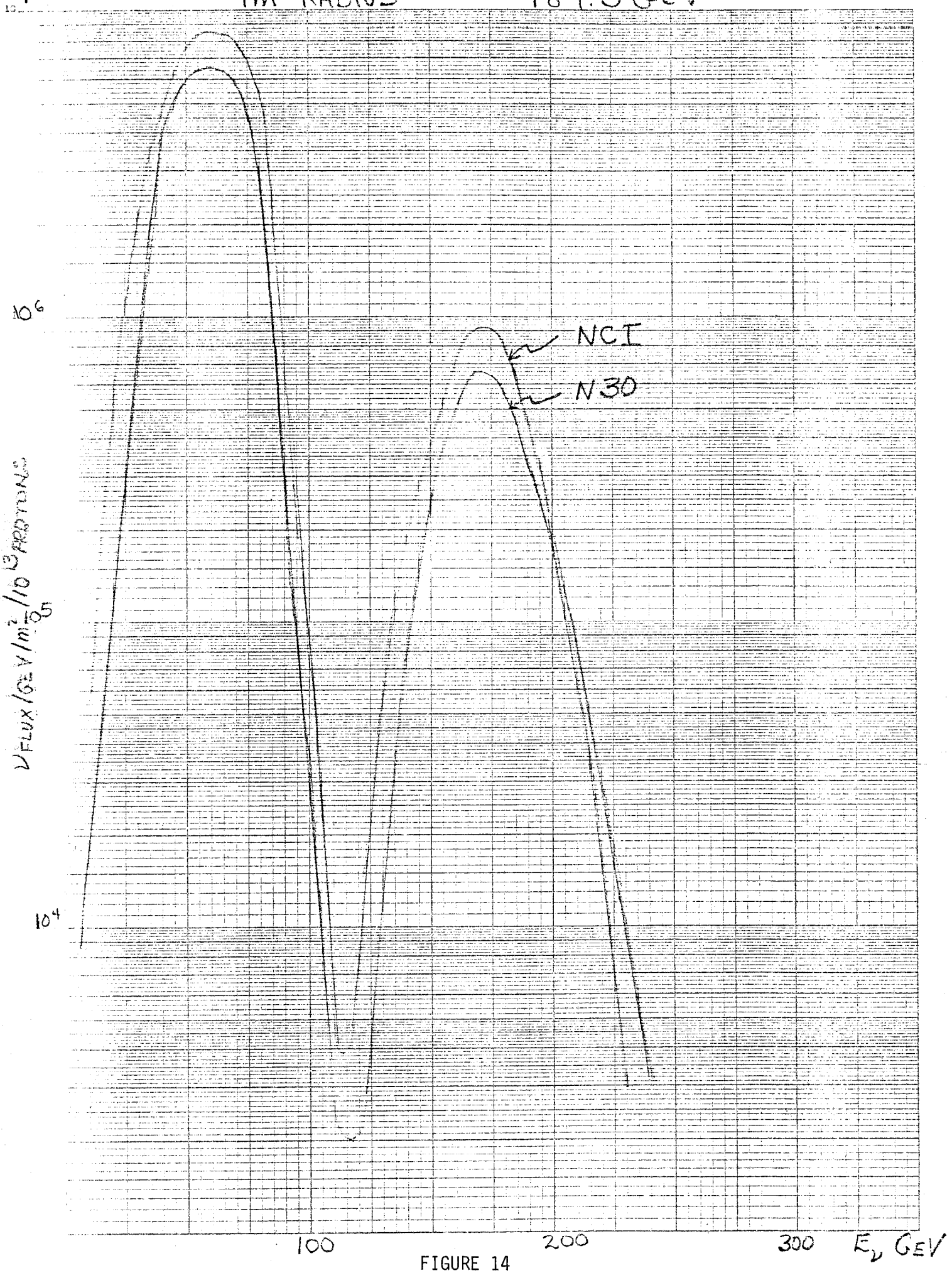
1m RADIUS
187.5 GeV
NCI
N30
10^6
10^4
ν_{FLUX} /GeV/m^2/10^{13} PROTONS
100
200
300
E_ν GEV

FIGURE 14

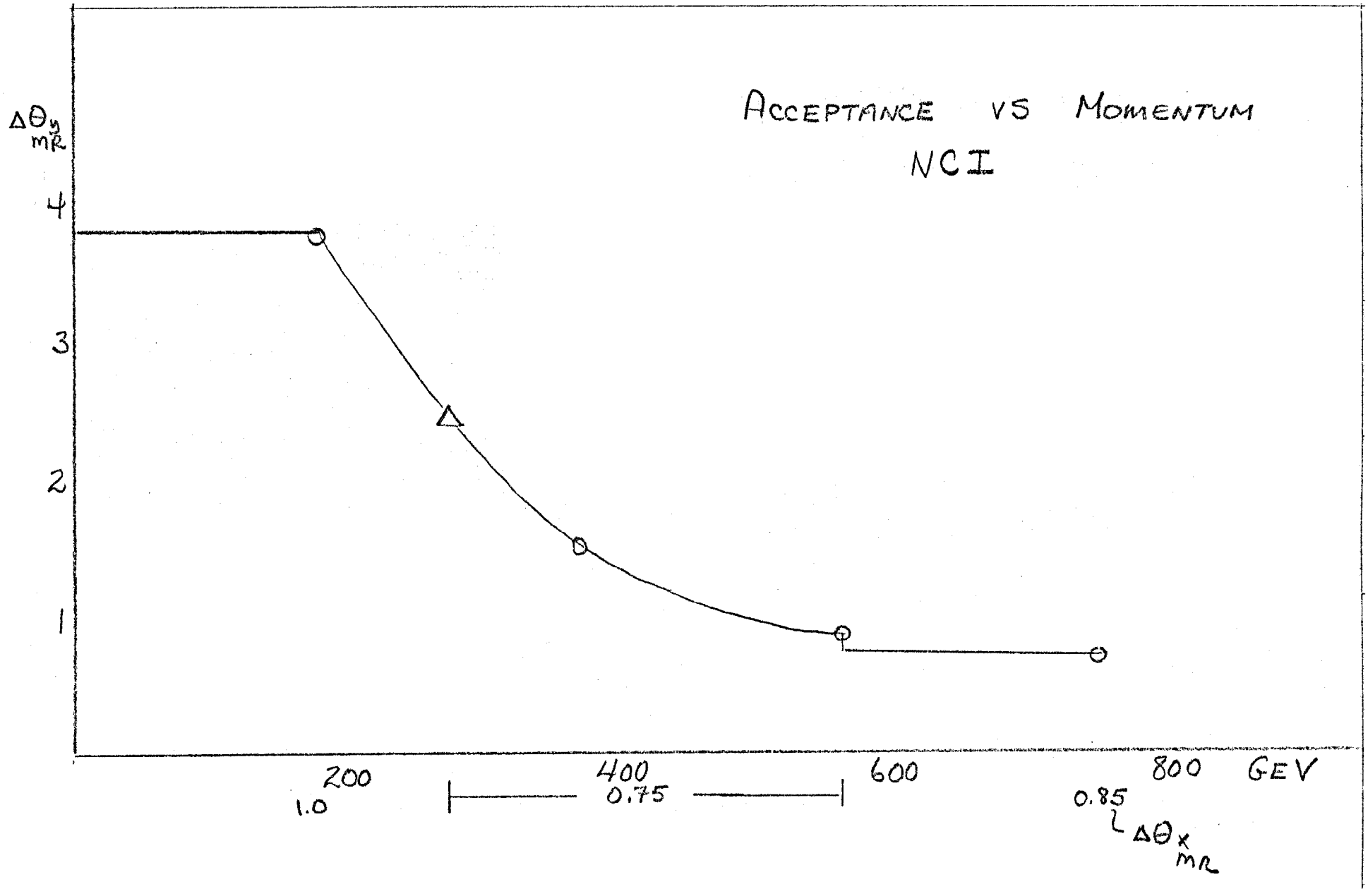
ACCEPTANCE VS MOMENTUM
NCI
$\Delta\theta_y$ mR
4
3
2
1
200
400
600
800
GEV
1.0
0.75
0.85
$\Delta\theta_x$ mR

FIGURE 15

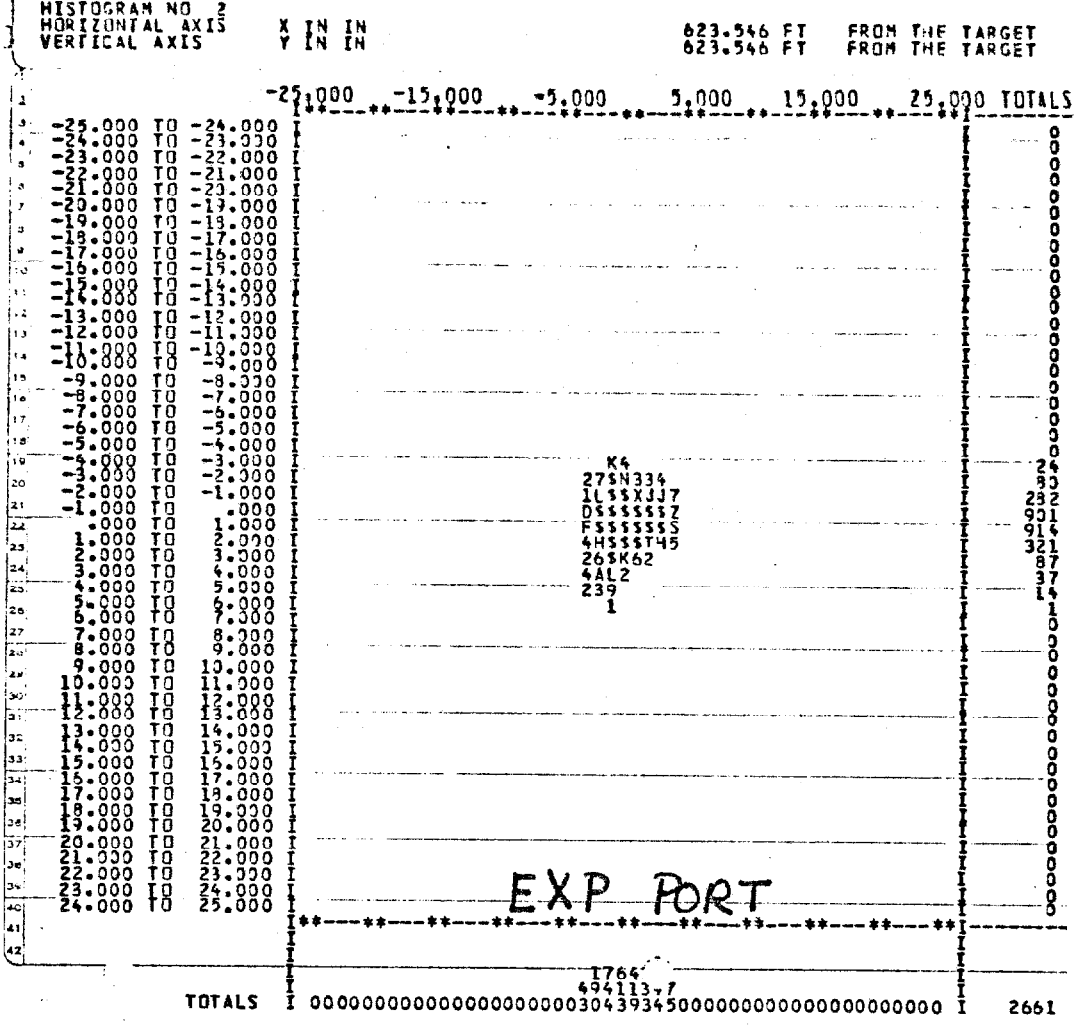

N3Ø

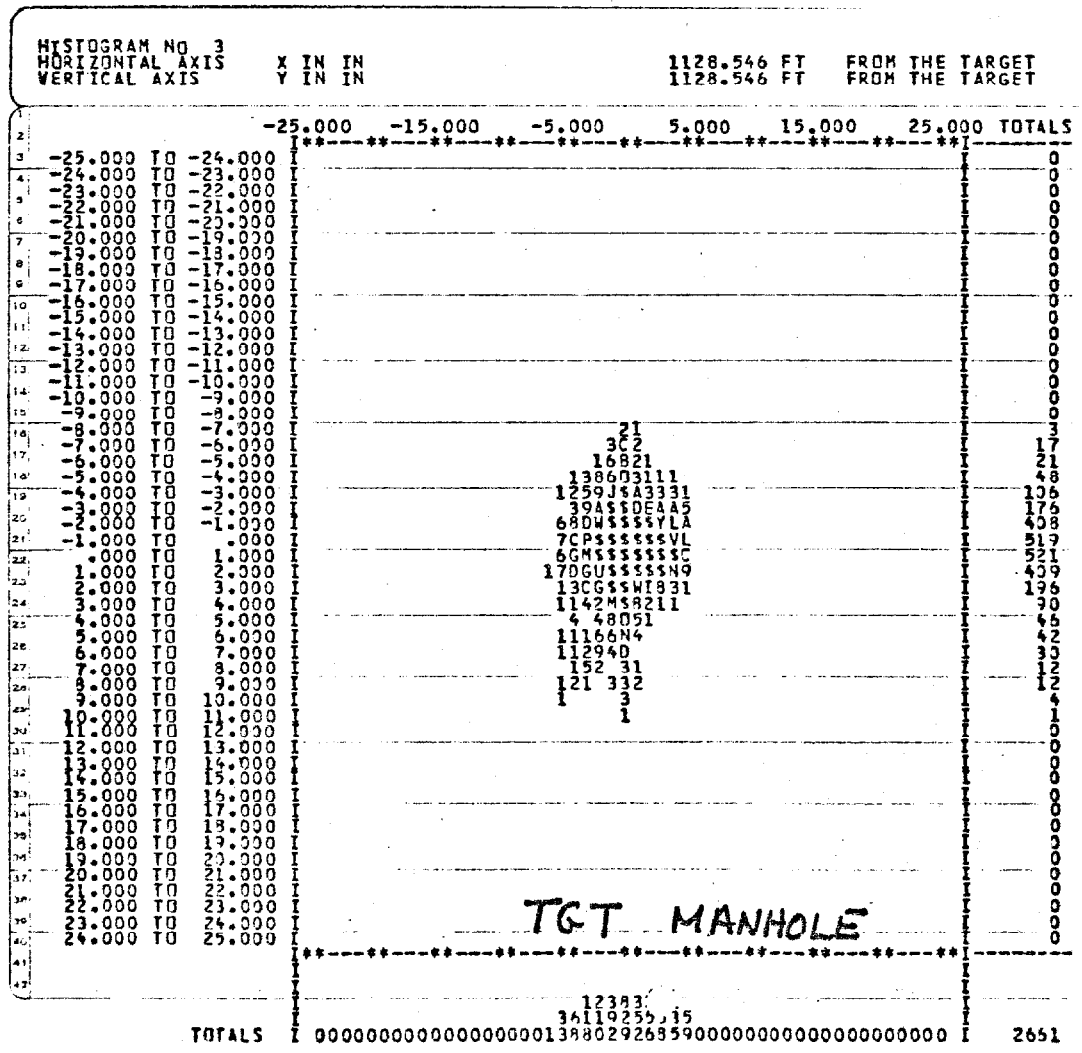

FIGURE 16

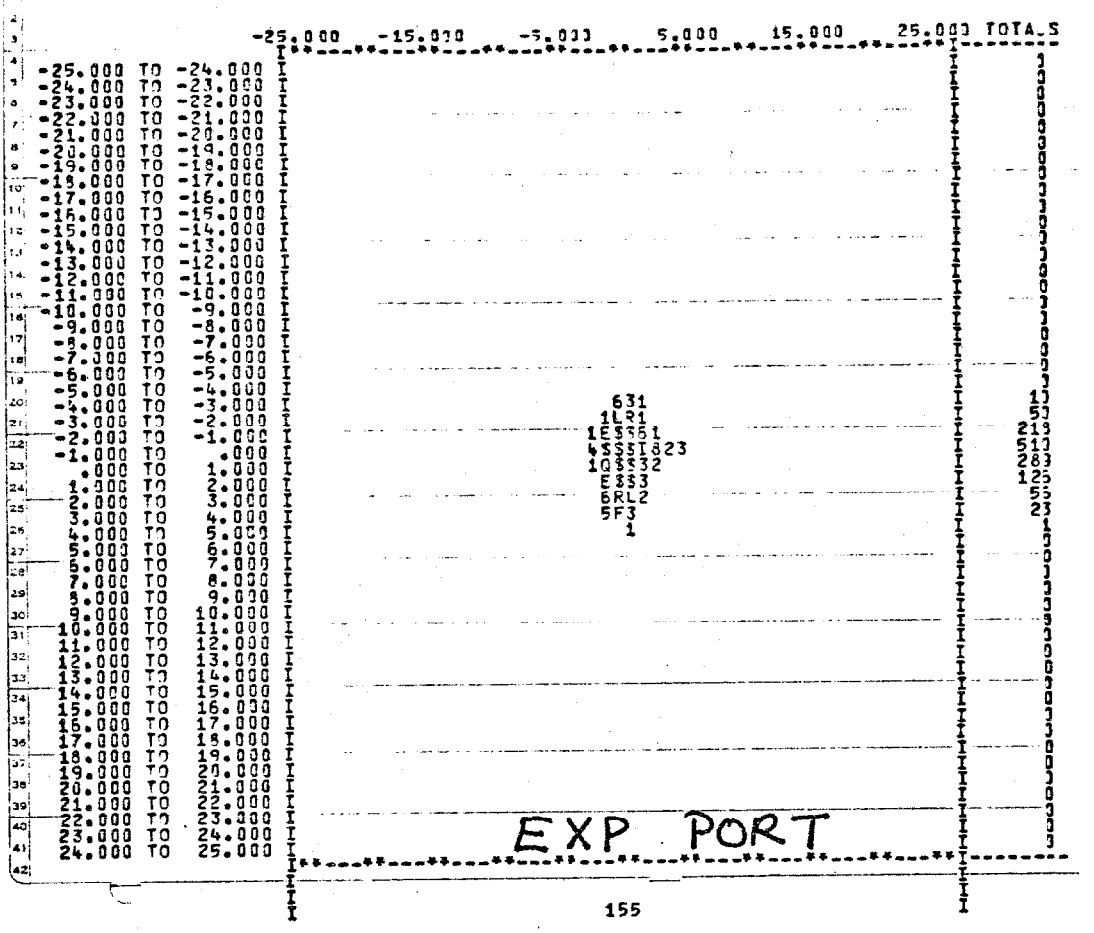

NCI

750

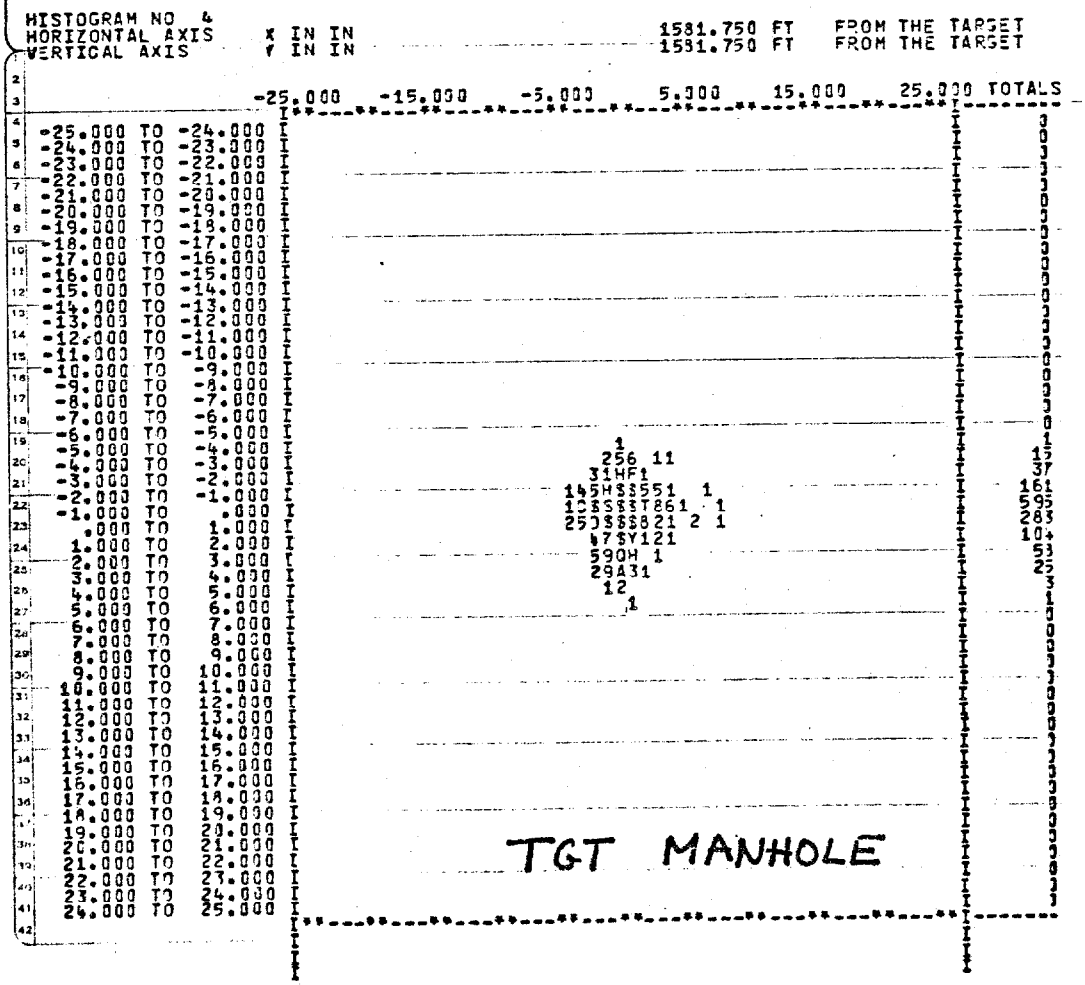

FIGURE 17A

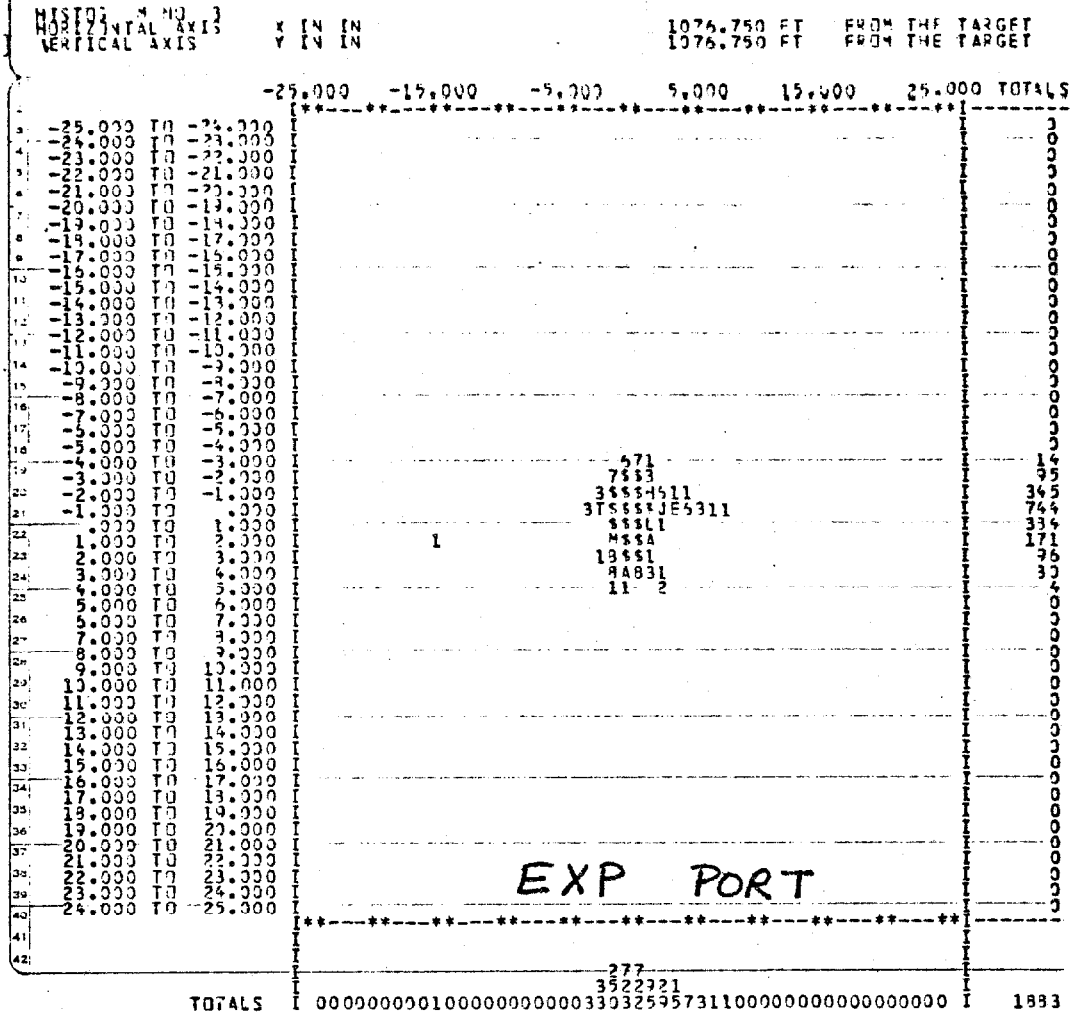

NCI
562

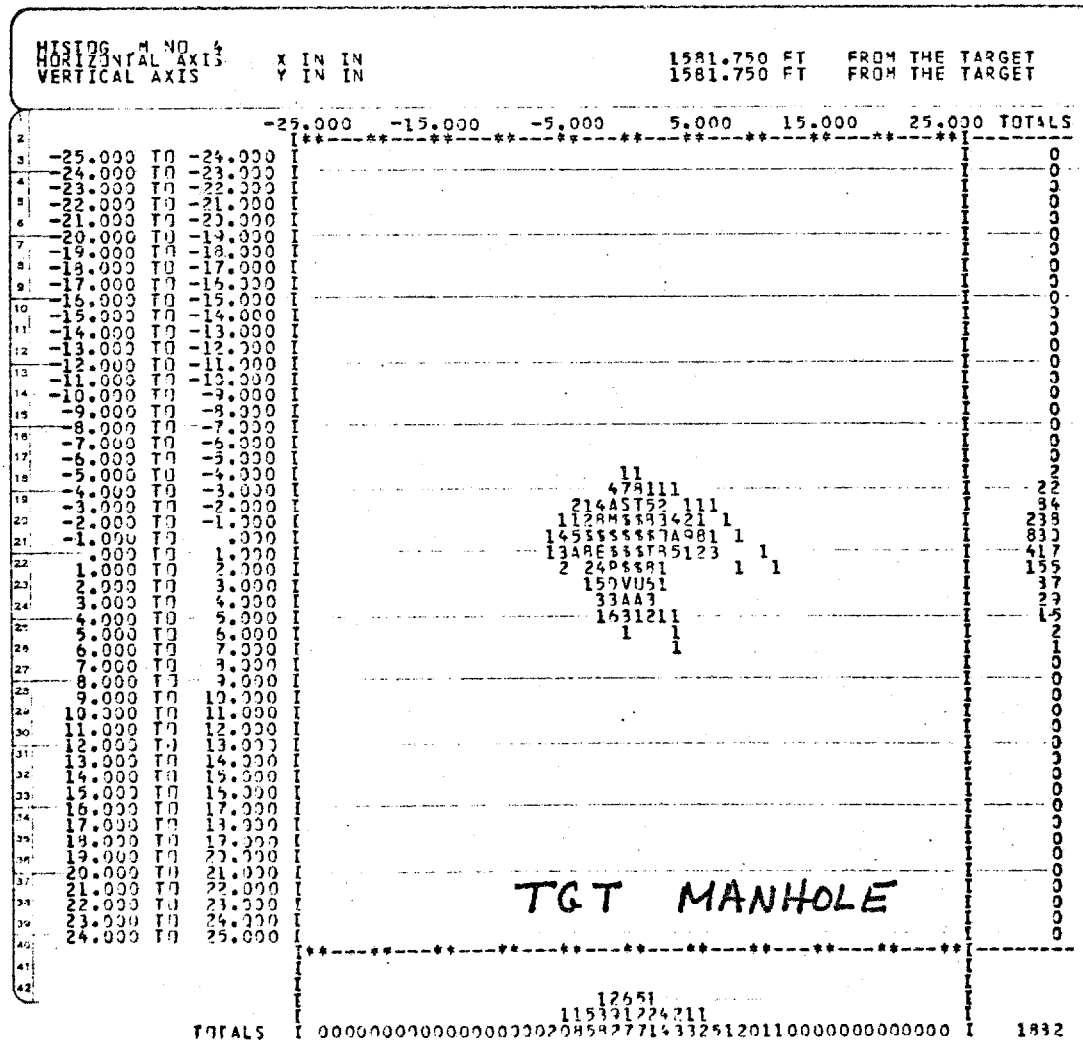

FIGURE 17B

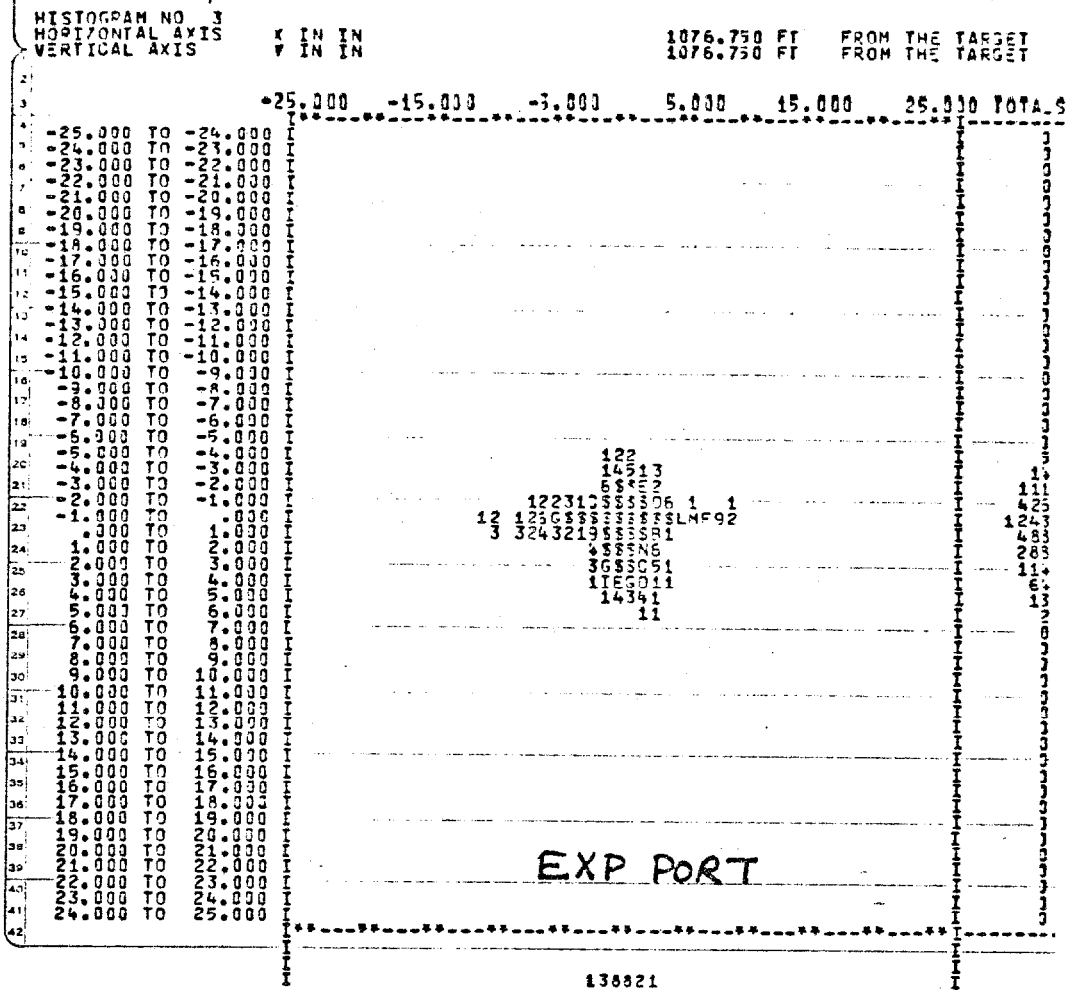

NCI
375

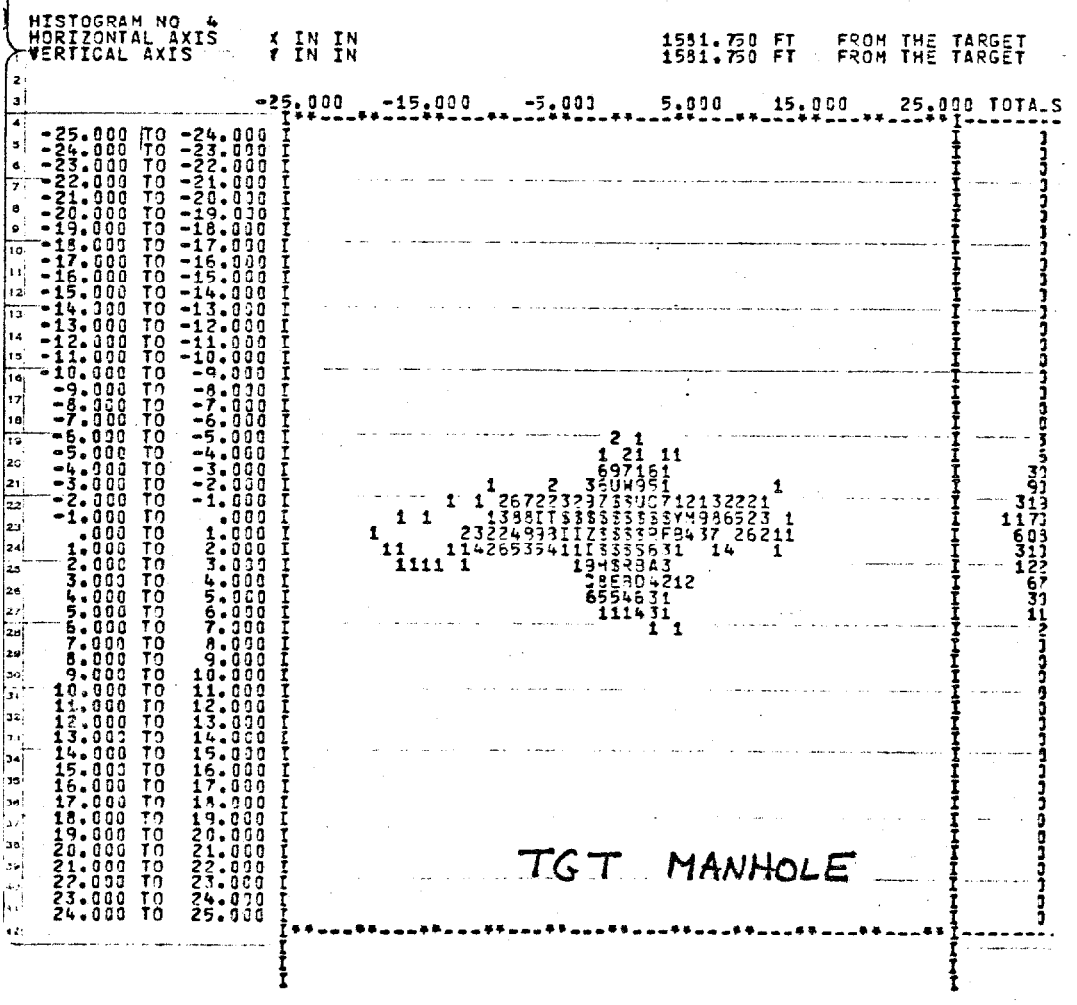

FIGURE 17C

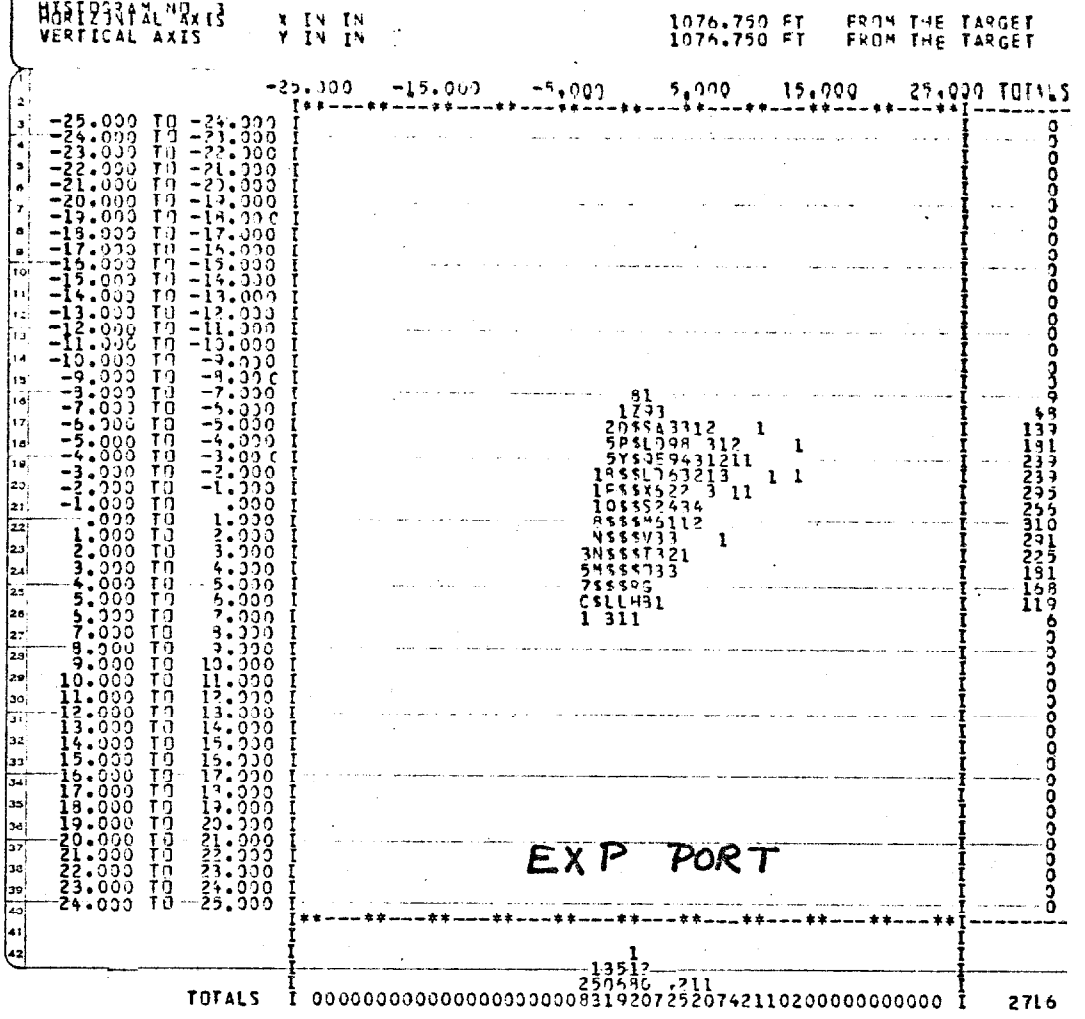

NC I
187

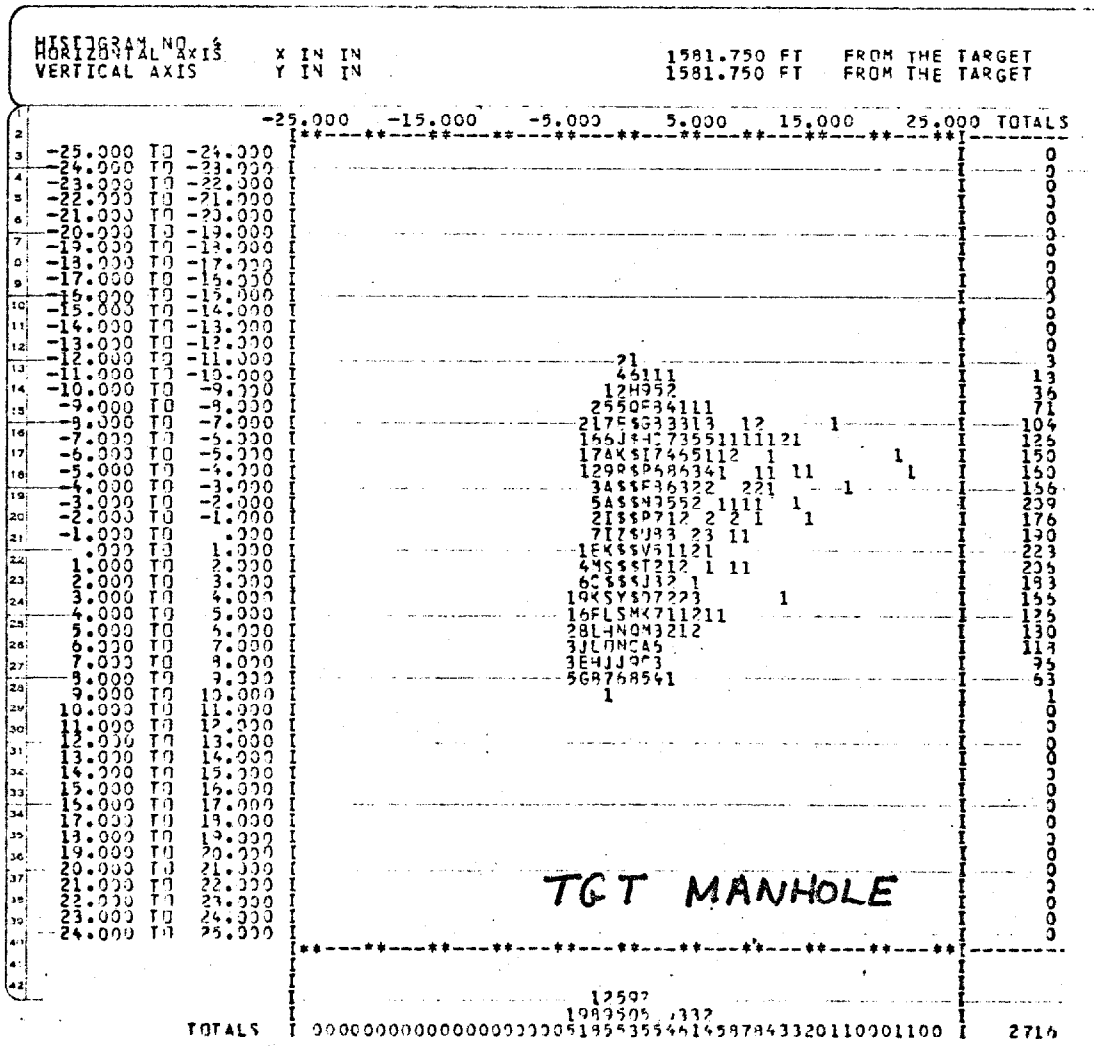

FIGURE 17D

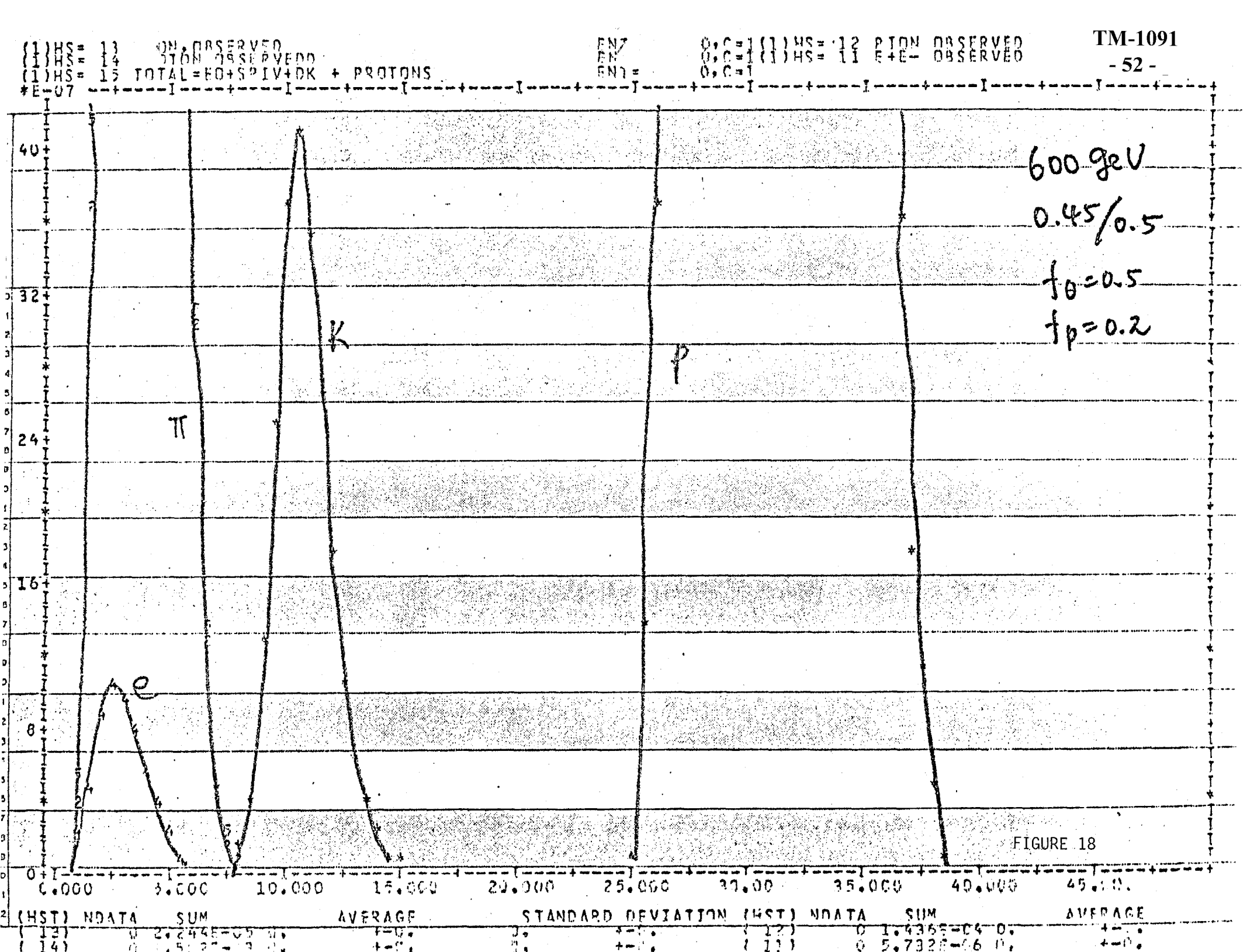
(1)HS= 13 ON.OBSERVED
(1)HS= 14 STON OBSERVED
(1)HS= 15 TOTAL=EO+SPIV+DK + PROTONS
ENT 0,C=1(1)HS= 12 PION OBSERVED
EN 0,C=1(1)HS= 11 E+E- OBSERVED
ENT= 0,C=1
*E-07
40
32
24
16
8
0
600 geV
0.45/0.5
f_θ=0.5
f_p=0.2
π
K
p
e
0.000
5.000
10.000
15.000
20.000
25.000
30.00
35.000
40.000
45.000
(HST) NDATA SUM AVERAGE STANDARD DEVIATION (HST) NDATA SUM AVERAGE
(13) 0 2.244E-05 0. +-0. 0. +-0. (12) 0 1.436E-04 0. +-0.
(14) 0 1.5[illegible] 0. +-0. 0. +-0. (11) 0 5.732E-06 0. +-0.

FIGURE 18

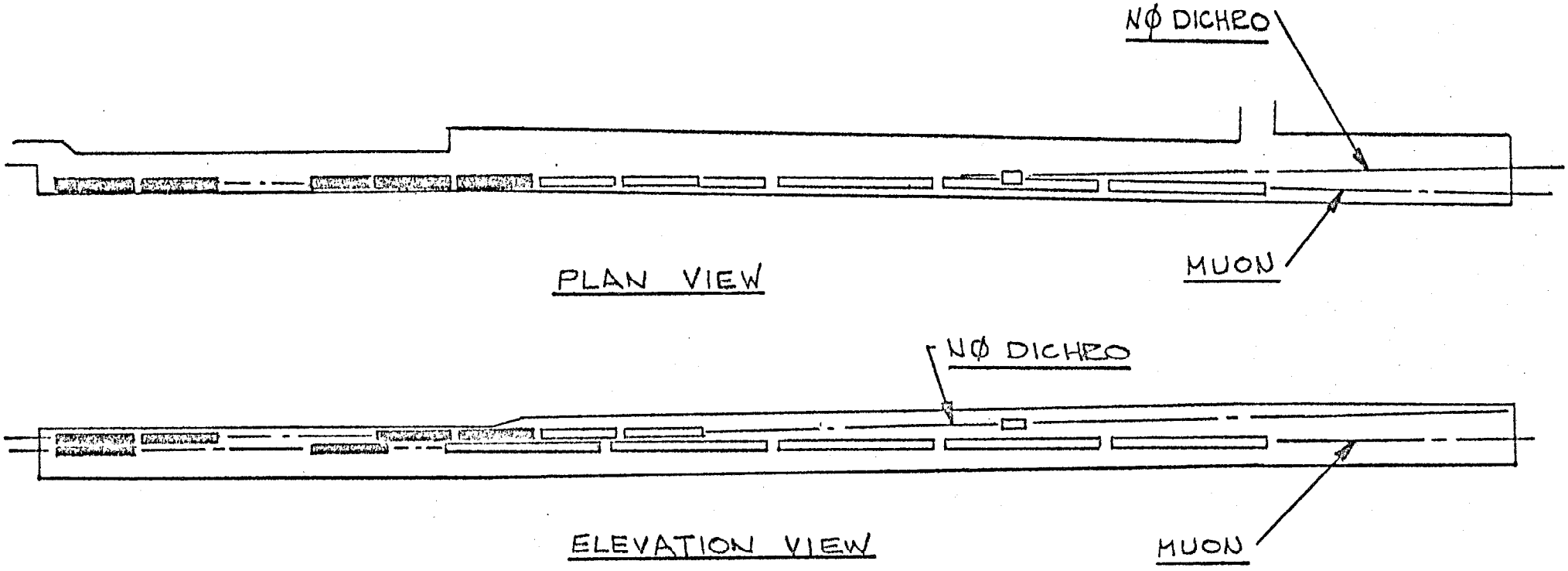
NØ DICHRO
MUON
PLAN VIEW
NØ DICHRO
MUON
ELEVATION VIEW
DIPOLE
QUAD
G-2

FIGURE 19

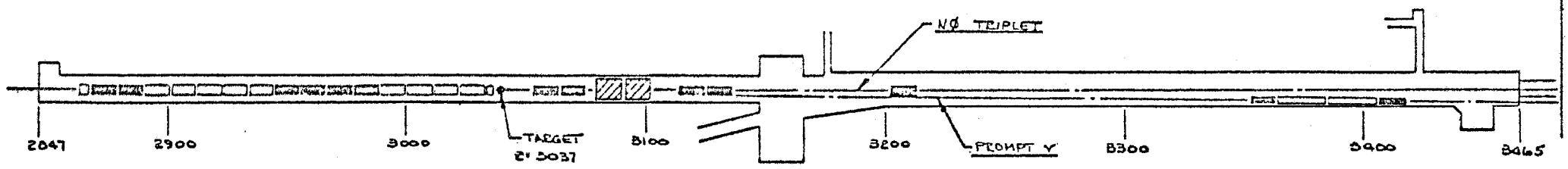

PLAN VIEW

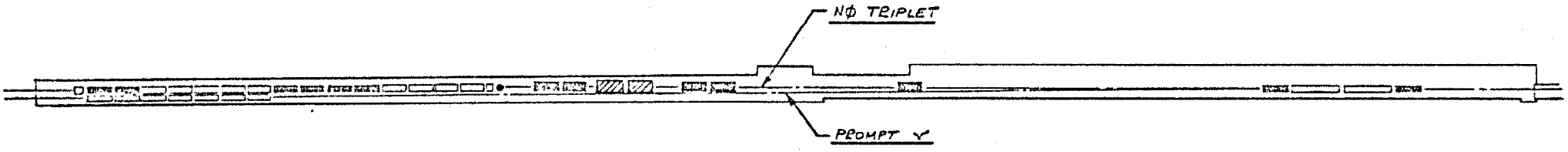

ELEVATION VIEW

FIGURE 20A

NØ TRIPLET & PROMPT

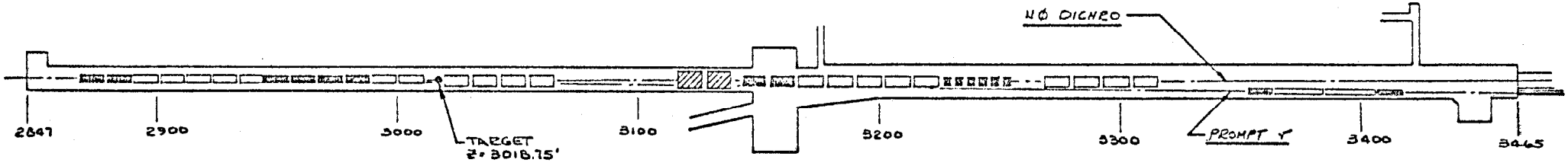

PLAN VIEW

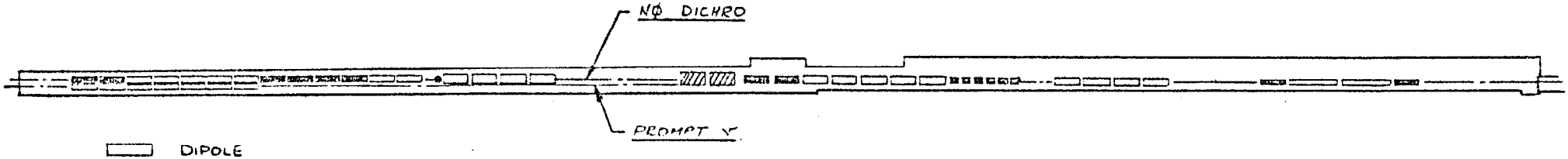

ELEVATION VIEW

FIGURE 20B

NØ DICHRO & PROMPT

FERMILAB
ENGINEERING NOTE

SECTION | PROJECT | SERIAL-CATEGORY | PAGE

SUBJECT N7, TRIPLET & N.B.
EQUIPMENT AT Z = 2890'

NAME H. STREDDE
DATE 10-15-81 | REVISION DATE

FLOOR ELEVATION = 738.995'

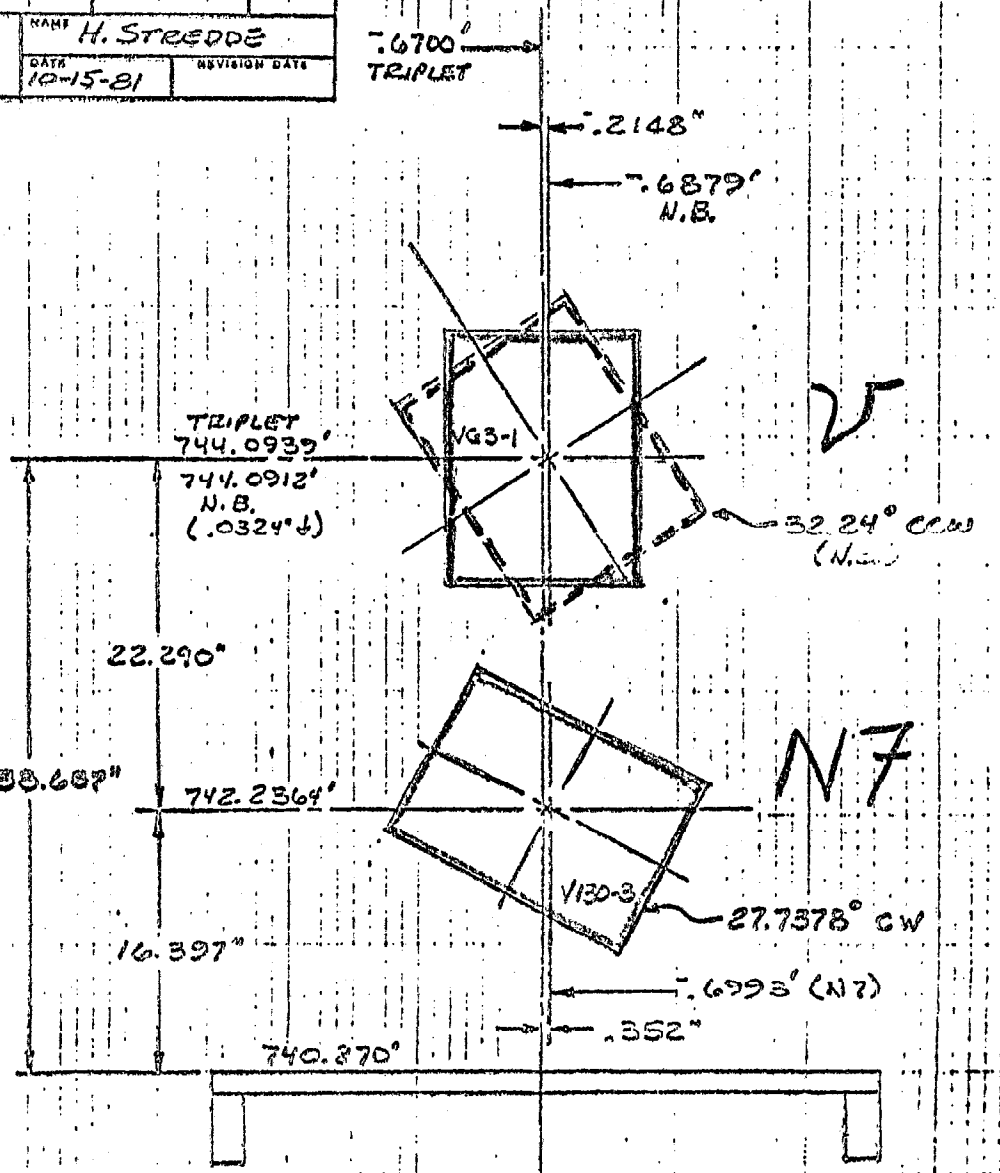

BEDPLATE & TRIPLET

FIGURE 21